

The Everchanging Pulsating White Dwarf GD358

S.O. Kepler¹, R. Edward Nather², Don E. Winget², Atsuko Nitta³, S. J. Kleinman³, Travis Metcalfe^{2,4}, Kazuhiro Sekiguchi⁵, Jiang Xiaojun⁶, Denis Sullivan⁷, Tiri Sullivan⁷, Rimvydas Janulis⁸, Edmund Meistas⁸, Romualdas Kalytis⁸, Jurek Krzesinski⁹, Waldemar Ogłóza⁹, Staszek Zola¹⁰, Darragh O'Donoghue¹¹, Encarni Romero-Colmenero¹¹, Peter Martinez¹¹, Stefan Dreizler¹², Jochen Deetjen¹², Thorsten Nagel¹², Sonja L. Schuh¹², Gerard Vauclair¹³, Fu Jian Ning¹³, Michel Chevreton¹⁴, Jan-Erik Solheim¹⁵, Jose M. Gonzalez Perez¹⁵, Frank Johannessen¹⁵, Antonio Kanaan¹⁶, José Eduardo Costa¹, Alex Fabiano Murillo Costa¹, Matt A. Wood¹⁷, Nicole Silvestri¹⁷, T.J. Ahrens¹⁷, Aaron Kyle Jones^{18,*}, Ansley E. Collins^{19,*}, Martha Boyer^{20,*}, J. S. Shaw²¹, Anjum Mukadam², Eric W. Klumpe²², Jesse Larrison²², Steve Kawaler²³, Reed Riddle²³, Ana Ulla²⁴, and Paul Bradley²⁵

¹ Instituto de Física da UFRGS, Porto Alegre, RS - Brazil e-mail: kepler@if.ufrgs.br

² Department of Astronomy & McDonald Observatory, University of Texas, Austin, TX 78712, USA

³ Sloan Digital Sky Survey, Apache Pt. Observatory, P.O. Box 59, Sunspot, NM 88349, USA

⁴ Harvard-Smithsonian Center for Astrophysics, 60 Garden Street, Cambridge, MA 02138 USA e-mail: travis@whitedwarf.org

⁵ Subaru National Astronomical Observatory of Japan e-mail: kaz@subaru.naoj.org

⁶ Beijing Astronomical Observatory, Academy of Sciences, Beijing 100080, China e-mail: jiang@astro.as.utexas.edu

⁷ University of Victoria, Wellington, New Zealand

⁸ Institute of Theoretical Physics and Astronomy, Gostauto 12, Vilnius 2600, Lithuania

⁹ Mt. Suhora Observatory, Cracow Pedagogical University, Ul. Podchorazych 2, 30-084 Cracow, Poland

¹⁰ Jagiellonian University, Krakow, Poland e-mail: zola@oa.uj.edu.pl

¹¹ South African Astronomical Observatory

¹² Universitat Tübingen, Germany

¹³ Université Paul Sabatier, Observatoire Midi-Pyrénées, CNRS/UMR5572, 14 av. E. Belin, 31400 Toulouse, France

¹⁴ Observatoire de Paris-Meudon, DAEC, 92195 Meudon, France e-mail: chevreton@obspm.fr

¹⁵ Institutt for fysikk, 9037 Tromsø, Norway

¹⁶ Departamento de Física, Universidade Federal de Santa Catarina, CP 476, CEP 88040-900, Florianópolis, Brazil, e-mail: kanaan@fsc.ufsc.br

¹⁷ Dept. of Physics and Space Sciences & The SARA Observatory, Florida Institute of Technology, Melbourne, FL 32901 *

¹⁸ University of Florida, 202 Nuclear Sciences Center Gainesville, FL 32611-8300

¹⁹ Johnson Space Center, 2101 NASA Road 1, Mail Code GT2, Houston, TX 77058, USA

²⁰ University of Minnesota, Department of Physics & Astronomy, 116 Church St. S.E., Minneapolis, MN 55455

²¹ University of Georgia at Athens, Department of Physics and Astronomy, Athens, GA 30602-2451, USA

²² Middle Tennessee State University, Department of Physics and Astronomy Murfreesboro, TN 37132, USA

²³ Department of Physics and Astronomy, Iowa State University, Ames, IA 50011, USA

²⁴ Universidade de Vigo, Depto. de Física Aplicada, Facultade de Ciencias, Campus Marcosende-Lagoas, 36200 Vigo (Pontevedra), Spain e-mail: ulla@uvigo.es

²⁵ Los Alamos National Laboratory, X-2, MS T-085 Los Alamos, NM 87545, USA

Received 6 Dec 2002 / Accepted 22 Jan 2003

Abstract. We report 323 hours of nearly uninterrupted time series photometric observations of the DBV star GD 358 acquired with the Whole Earth Telescope (WET) during May 23rd to June 8th, 2000. We acquired more than 232 000 independent measurements. We also report on 48 hours of time-series photometric observations in Aug 1996. We detected the non-radial g-modes consistent with degree $\ell = 1$ and radial order 8 to 20 and their linear combinations up to 6th order. We also detect, for the first time, a high amplitude $\ell = 2$ mode, with a period of 796 s. In the 2000 WET data, the largest amplitude modes are similar to those detected with the WET observations of 1990 and 1994, but the highest combination order previously detected was 4th order. At one point

during the 1996 observations, most of the pulsation energy was transferred into the radial order $k = 8$ mode, which displayed a sinusoidal pulse shape in spite of the large amplitude. The multiplet structure of the individual modes changes from year to year, and during the 2000 observations only the $k = 9$ mode displays clear normal triplet structure. Even though the pulsation amplitudes change on timescales of days and years, the eigenfrequencies remain essentially the same, showing the stellar structure is not changing on any dynamical timescale.

Key words. (Stars:) white dwarfs, Stars: variables: general, Stars: oscillations, Stars: individual: GD 358, Stars: evolution

1. Introduction

GD 358, also called V777 Herculis, is the prototype of the DBV class of white dwarf pulsators. It was the first pulsating star detected based on a theoretical prediction (Winget et al. 1985), and is the pulsating star with the largest number of periodicities detected after the Sun. Detecting as many modes as possible is important, as each periodicity detected yields an independent constraint on the star’s structure. The study of pulsating white dwarf stars has allowed us to measure the stellar mass and composition layers, to probe the physics at high densities, including crystallization, and has provided a chronometer to measure the age of the oldest stars and consequently, the age of the Galaxy.

Robinson, Kepler & Nather (1982) and Kepler (1984) demonstrated that the variable white dwarf stars pulsate in non-radial gravity modes. Beauchamp et al. (1999) studied the spectra of the pulsating DBs to determine their instability strip at $22\,400 \leq T_{\text{eff}} \leq 27\,800$ K, and found $T_{\text{eff}} = 24\,900$ K, $\log g = 7.91$ for the brightest DBV, GD 358 ($V=13.85$), assuming no photospheric H, as confirmed by Provencal et al. (2000). Provencal et al. studied the HST and EUVE spectra, deriving $T_{\text{eff}} = 27\,000 \pm 1\,000$ K, finding traces of carbon in the atmosphere [$\log(\text{C}/\text{He}) = -5.9 \pm 0.3$] and a broadening corresponding to $v \sin i = 60 \pm 6$ km/s. They also detected Ly α that is probably interstellar. Althaus & Benvenuto (1997) demonstrated that the Canuto, Goldman, & Mazzitelli (1996, hereafter CGM) self consistent theory of turbulent convection is consistent with the $T_{\text{eff}} \simeq 27\,000$ K determination, as GD 358 defines the blue edge of the DBV instability strip. Shipman et al. (2002) extended the blue edge of the DBV instability strip by finding that the even hotter star PG0112+104 is a pulsator.

Winget et al. (1994) reported on the analysis of 154 hours of nearly continuous time series photometry on GD 358, obtained during the Whole Earth Telescope (WET) run of May 1990. The Fourier temporal spectrum of the light curve is dominated by periodicities in the range $1000 - 2400 \mu\text{Hz}$, with more than 180 significant peaks. They identify all of the triplet frequencies as having degree $\ell = 1$ and, from the details of their triplet (k) spacings, from which Bradley & Winget (1994) derived the total stellar mass as $0.61 \pm 0.03 M_{\odot}$, the mass of the outer helium envelope as $2.0 \pm 1.0 \times 10^{-6} M_{*}$, the luminosity as $0.050 \pm 0.012 L_{\odot}$ and, deriving a temperature and bolometric correction, the distance as 42 ± 3 pc. Winget et al. (1994) found changes in the m spacings among the triplet modes, and by assuming the rotational splitting coefficient $C_{\ell,k}(r)$ depends only on radial overtone k and the rotation angular velocity $\Omega(r)$, interpret the observed spacing as strong evidence of radial differential rotation, with the outer envelope rotating some 1.8 times faster than the core. However, Kawaler, Sekii, & Gough (1999) find that the core rotates faster than the envelope when they perform rotational splitting inversions of the observational data. The apparently contradictory result is due to the presence of mode trapping and the behavior of the rotational splitting kernel in the core of the model. Winget et al. also found significant power at the sums and differences of the dominant frequencies, indicating that non-linear processes are significant, but with a richness and complexity that rules out resonant mode coupling as a major cause.

We show that in the WET data set reported here (acquired in 2000), only 12 of the periodicities can be identified as independent g-mode pulsations, probably all different radial overtones (k) with same spherical degree $\ell = 1$, plus the azimuthal m components for $k = 8$ and 9. The high amplitude with a period of 796 s is identified as an $\ell = 2$ mode; it was not present in the previous data sets. Most, if not all, of the remaining periodicities are linear combination peaks of these pulsations. Considering there are many more observed combination frequencies than available eigenmodes, we interpret the linear combination peaks as caused by non-linear effects, not real pulsations. This interpretation is consistent with the proposal by Brickhill (1992) and Wu (2001) that the combination frequencies appear by the non-linear response of the medium. Recently, van Kerkwijk et al. (2000) and Clemens et al. (2000) show that most linear combination peaks for the DAV G29-38 do not show any velocity variations, while the eigenmodes do. However, Thompson et al. (2003) argue that some combination peaks do show velocity variations.

As a clear demonstration of the power of asteroseismology, Metcalfe, Winget, & Charbonneau (2001) and Metcalfe, Salaris, & Winget (2002) used GD 358 observed periods from Winget et al. (1994) and a genetic algorithm to search for the optimum theoretical model with static diffusion envelopes, and constrained the $^{12}\text{C}(\alpha, \gamma)^{16}\text{O}$ cross section, a crucial

Send offprint requests to: S.O. Kepler, e-mail: kepler@if.ufrgs.br

* Southeastern Association for Research in Astronomy (SARA) NSF-REU Student.

parameter for many fields in astrophysics and difficult to constrain in terrestrial laboratories. Montgomery, Metcalfe, & Winget (2001) also used the observed pulsations to constrain the diffusion of ${}^3\text{He}$ in white dwarf stars. They show their best model for GD 358 has O/C/ ${}^4\text{He}$ / ${}^3\text{He}$ structure, $T_{\text{eff}} = 22\,300 \pm 500$ K, $M_* = 0.630 \pm 0.015 M_{\odot}$, a thick He layer, $\log M({}^4\text{He})/M_* = (-2.79 \pm 0.06)$, distinct from the thin layer, $\log M({}^4\text{He})/M_* = (-5.70 \pm {}^{+0.18}_{-0.30})$, proposed by Bradley & Winget (1994). Montgomery, Metcalfe, & Winget’s model had $\log M({}^3\text{He})/M_* = (-7.49 \pm 0.12)$, but Wolff et al. (2002) did not detect any ${}^3\text{He}$ in the spectra of all the DBs they observed. On the other hand, Dehner & Kawaler (1995), Brassard & Fontaine (2002), and Fontaine & Brassard (2002) show that a thin helium envelope is consistent with the evolutionary models starting at PG1159 models and ending as DQs, as diffusion is still ongoing around 25 000K and lower temperatures. Therefore there could be two transition zones in the envelope, one between the He envelope and the He/C/O layer, where diffusion is still separating the elements, and another transition between this layer and the C/O core.

Gautschy & Althaus (2002) calculated nonadiabatic pulsation properties of DB pulsators using evolutionary models including the CGM full-spectrum turbulence theory of convection and time-dependent element diffusion. They show that up to 45 dipole modes should be excited, with periods between 335s and 2600s depending on the mass of the star, though their models did not include pulsation–convection coupling. They obtain a trapping-cycle length of $\Delta k = 5 \rightarrow 7$, and the quadrupole modes showed instabilities comparable to the dipole modes.

Buchler, Goupil, & Hansen (1997) show that if there is a resonance between pulsation modes, even if the mode is stable, its amplitude will be necessarily nonzero. They also point out that in case of amplitude saturation, it is the smaller adjacent modes that show the largest amplitude variation, not the main modes. However, if the combination peaks are not real modes in a physical sense, just non-linear distortion by the medium, it is not clear that one would have resonant (mode-coupling) between the combination peaks and real modes.

When the Whole Earth Telescope observed GD 358 in 1990, 181 periodicities were detected, but only modes from radial order $k = 8$ to 18 were identified, most of them showing triplets, consistent with the degree $\ell = 1$ identification. In fact, the observed period spacing is consistent with the measured parallax only if the observed pulsations have degree $\ell = 1$ (Bradley & Winget 1994).

Vuille et al. (2000) studied the 342 hours of Whole Earth Telescope data obtained in 1994, showing again modes with $k = 8$ to 18, and discovered up to 4th-order cross-frequencies in the power spectra. They compared the amplitudes and phases observed with those predicted by the pulsation–convection interaction proposed by Brickhill (1992), and found reasonable agreement.

Note that the number of nodes in the radial direction k cannot be determined observationally and rely on a detailed comparison of the observed periods with those predicted by pulsation models.

2. Observations

We report here two data sets: 48 hr of time series photometry acquired in August 1996, with the journal of observations presented in Table 1. The second data set consists of 323 hours acquired in May–June 2000 (see Tables 2 and 3 for the observing log). Both of these data sets were obtained simultaneously with time resolved STIS spectroscopy with the Hubble Space Telescope, which will be reported elsewhere.

In 1996, the observations were obtained with three channel time series photometry using bi-alkali photocathodes (Kleinman, Nather, & Phillips, 1996), in Texas, China, and Poland. During 23 May to 23 June, 2000, we observed GD 358 mainly with two and three channel time series photometers using bi-alkali photocathodes and a time resolution of 5 s. The May–June 2002 run used 13 telescopes composing the Whole Earth Telescope. The telescopes, ranging from 60 cm to 256 cm in diameter, were located in Texas, Arizona, Hawaii, New Zealand, China, Lithuania, Poland, South Africa, France, Spain, Canary Islands, and Brazil. As the pulsations in white dwarf stars are in phase at different wavelengths (Robinson, Kepler, & Nather 1982), we used no filters, to maximize the detected signal.

Each run was reduced and analyzed as described by Nather et al. (1990) and Kepler (1993), correcting for extinction through an estimated local coefficient, and sky variations measured continuously on three channel and CCD observations, or sampled frequently on two channel photometers. The second channel of the photometer monitored a nearby star to assure photometric conditions or correct for small non-photometric conditions. The CCD measurements were obtained with different cameras which are not described in detail here. At least two comparison stars were in each frame and allowed for differential weighted aperture photometry. The consecutive data points were 10 to 30 s apart, depending if the CCDs were frame transfer or not.

After this preliminary reduction, we brought the data to the same fractional amplitude scale and converted the middle of integration times to Barycentric Coordinated Time TCB (Standish 1998). We then computed a Discrete Fourier Transform (DFT) for the combined 2000 data, shown in Fig. 1. Due to poor weather conditions during the run, our coverage is not continuous, causing gaps in the observed light curve; these gaps produce aliases in the Fourier transform. At the bottom of Fig. (1) we present the spectral window, the Fourier transform of a single sinusoid sampled exactly as the real data. It shows the pattern of peaks each individual frequency in the data introduces in the DFT.

Telescope	Run	Date (UT)	Start Time(UT)	Length (s)
Suhora 60 cm	suh-55	Aug 10	23:28:00	8890
Suhora 60 cm	suh-56	Aug 12	20:26:40	14730
McDonald 210 cm	an-0036	Aug 13	3:06:30	13840
Suhora 60 cm	suh-57	Aug 13	19:12:10	22050
McDonald 210 cm	an-0038	Aug 14	3:14:10	12920
BAO 85 cm	bao-0026	Aug 14	13:10:00	13610
Suhora 60 cm	suh-58	Aug 14	23:19:10	5370
McDonald 210 cm	an-0040	Aug 15	3:04:30	15780
McDonald 96 cm	an-0041	Aug 16	2:54:00	15700
BAO 85 cm	bao-0027	Aug 16	13:01:50	1250
BAO 85 cm	bao-0028	Aug 16	13:42:30	9330
McDonald 96 cm	an-0042	Aug 17	5:01:50	6420
McDonald 96 cm	an-0043	Aug 18	4:05:30	3930
Suhora 60-cm	suh-59	Aug 18	21:02:10	13010
McDonald 96 cm	an-0042	Aug 18	4:05:30	3930
McDonald 96 cm	an-0043	Aug 19	2:44:40	2100
McDonald 96 cm	an-0044	Aug 19	2:44:40	2100
McDonald 96 cm	an-0044	Aug 19	3:47:00	4250
McDonald 96 cm	an-0045	Aug 19	3:47:00	4250
McDonald 96 cm	an-0046	Aug 19	4:58:30	7160
Suhora 60 cm	suh-60	Aug 19	20:28:00	15290
Suhora 60 cm	suh-61	Aug 20	21:04:00	10670

Table 1. Journal of ground-based observation for GD358 in August, 1996.

The Fourier spectra displayed in Fig. (1) looks similar to the ones obtained in 1990 and 1994 (see Figure 2), but the amplitude of all the modes changed significantly. As we describe in more detail later, the most striking feature of the 2000 data is the absence of triplets, except for $k = 9$. The 1996 data are even more unusual than the WET runs due to the observation of amplitude changes over an unprecedented short time. We describe these observations in more detail in section 3. We then describe the 2000 observations and our interpretations of them in Sections 4 through 7.

3. Changes in the Dominant Mode in 1996

We observed GD 358 in August 1996 to provide simultaneous observations to compare to HST time resolved spectroscopy made on August 16. The 1996 data covers 10 days of the most remarkable amplitude behavior ever seen in a pulsating white dwarf. Observing this behavior is serendipitous, as individual observers and the WET have observed GD 358 off and on for 20 years without seeing this sort of behavior.

Figure 3 shows how the amplitude of the $k = 8$ $P = 423$ s mode changed with time during our observations in August 1996. The amplitude changes we saw in our optical data are unprecedented in the observations of pulsating white dwarf stars; no report has been made of such a large amplitude variation in such a short amount of time. Here we describe what we found in our data.

The lightcurves acquired in August 1996 are displayed in Fig. 4 and the Fourier transform for each lightcurve is shown in Figure 4. Those in the first and second panels of Fig. 4 look very different from each other. The Fourier transform of the lightcurve from the first panel is similar to that from the 1994 WET data where we identified over 100 individual periodicities, while the Fourier transform of the second panel is dominated by only a single periodicity (Fig. 5); this represents a complete change in the mode structure, as well as the period of the dominant mode, in about one day!

In run an-0034, the $k = 8$ $P=423$ s mode’s amplitude is 170 mma, which is the largest amplitude we have ever seen for this mode. To check for additional pulsation power (perhaps lower amplitude pulsations dwarfed by the 423 s mode power), we prewhitened the an-0034 lightcurve by the 423 s mode. Prewhitening subtracts a sinusoid with a specified amplitude, phase and period from the original lightcurve, and it helps us look for smaller amplitude pulsations by eliminating the alias pattern of the dominant pulsation mode from the Fourier transform. In Fig. 6, we show the Fourier transform of the an-0034 lightcurve both before and after prewhitening. We see now that GD 358 was indeed dominated entirely by a single mode at a different period from the dominant mode a day earlier. We refer to this event by the musical term “*forte*”, or more informally as the “whoopsie”.

Given the spectacular behavior of GD 358 in August 1996, we obtained follow-up observations in September 1996 and April 1997. Table 4 shows the journal of observations for the September 1996 and April 1997 data. The lightcurve

Table 2. Journal of ground-based observation for GD358 in May-June, 2000.

Run Name	Telescope	Date (UT) (UT)	Start Time (s)	Length	
jr0523	Moletai 1.65m	May 23 00	22:15:49	6360	
tsm-0074	McDonald 2.1m	May 24	4:59:00	20050	
jr0524	Moletai 1.65m	May 24	20:24:35	10255	
tsm-0075	McDonald 2.1m	May 25	3:25:00	25440	
suh-089	SUHORA 0.6m	May 25	23:58:30	4715	
tsm-0076	McDonald 2.1m	May 26	3:18:30	25350	
suh-090	Suhora 0.6m	May 26	20:07:20	18995	
jr0526	Moletai 1.65m	May 26	20:26:00	12545	
teide02	Tenerife IAC 0.8m	May 27	01:25:20	13270	
tsm-0077	McDonald 2.1m	May 27	03:00:00	26100	
suh-091	Suhora 0.6m	May 27	19:56:20	15240	
sa-et1	SAAO 0.75m	May 28	00:18:30	15220	
teide04	Tenerife IAC 0.8m	May 28	0:37:10	14870	
tsm-0078	McDonald 2.1m	May 28	2:51:00	29040	
teide05	Tenerife IAC 0.8m	May 28	21:53:20	24700	
jr0528	Moletai 1.65m	May 28	20:28:20	9550	
tsm-0079	McDonald 2.1m	May 29	2:50:00	27300	
calto2905	Calar Alto 1.23m	May 29	21:20:00	6000	CCD
teide06	Tenerife IAC 0.8m	May 29	22:01:50	4375	
gv-2905	OHP	May 29	22:06:00	15530	
teide07	Tenerife IAC 0.8m	May 29	23:28:00	11460	
teide08	Tenerife IAC 0.8m	May 30	2:50:50	6850	
tsm-0080	McDonald 2.1m	May 30	3:00:00	28200	
suh-092	Suhora 0.6m	May 30	20:39:30	14880	
gv-2906	OHP 1.93m	May 30	20:44:00	4340	
teide09	Tenerife IAC 0.8m	May 30	21:58:50	25270	
sjk-0401	Hawaii UH 0.6m	May 31	7:19:00	26615	
gv-2907	OHP, 1.93 m	May 31	20:44:00	20400	
teide10	Tenerife IAC 0.8m	May 31	22:25:20	8195	
calto3105	Calar Alto 1.23m	May 31	21:30:00	5560	CCD
sa-od033	SAAO 0.75m	May 31	22:31:00	4000	
sjk-0402	Hawaii UH 0.6m	Jun 1	6:05:00	31265	
jxj-0103	BAO 0.85m	Jun 1	13:18:20	6950	
suh-093	Suhora 0.6m	Jun 1	19:55:30	19310	
jr0601	Moletai 1.65m	Jun 1	20:12:00	13145	
sa-od035	SAAO 0.75m	Jun 1	20:22:00	10600	
calto0106	Calar Alto 1.23m	Jun 1	20:46:00	4845	CCD
gv-2908	OHP 1.93m	Jun 1	20:48:00	19650	
teide11	Tenerife IAC 0.8m	Jun 1	22:38:40	2230	
teide12	Tenerife IAC 0.8m	Jun 1	23:16:20	12460	
tsm-0081	McDonald 2.1m	Jun 2	2:50:00	24000	
teide13	Tenerife IAC 0.8m	Jun 2	3:00:20	7180	
sara030	Sara 0.9m	Jun 2	8:30:00	14400	CCD
sjk-0403	Hawaii UH 0.6m	Jun 2	6:04:00	32505	
jxj-0003	BAAO 0.85m	Jun 2	15:24:50	11030	
suh-094	Suhora 0.6m	Jun 2	19:53:00	19530	
gv-2909	OHP 1.93m	Jun 2	21:40:00	16750	
jr0602	Moletai 1.65m	Jun 2	22:03:45	4740	
calto0602	Calar Alto 1.23m	Jun 2	23:20:00	4030	CCD
teide15	Tenerife IAC 0.8m	Jun 3	00:22:40	16630	

and the power spectrum during these observations (Fig. 7) seem to have returned to the more or less normal state seen in the past (Fig. 2), not the unusually high amplitude state it was in in August 1996 (Fig. 5).

We show the lightcurves of GD 358 at three different times in Fig. 8. The middle panel shows the lightcurve when the amplitude of the 423 s mode was at its largest. The lightcurve looks almost sinusoidal, with the single 423 s mode in the power spectrum. The result of this is that we obtain similar values for the peak-to-peak semi-amplitudes and the FT amplitude of the 423 s mode; this implies that a single spherical harmonic is a good representation of the stellar

Table 3. Journal of ground-based observation for GD358 in May-June, 2000. (cont.)

Run Name	Telescope	Date (UT)	Start Time (UT)	Length (s)	
calto0602.2	Calar Alto 1.23m	Jun 3	00:35:00	2800	
tsm-0082	McDonald 2.1m	Jun 3	3:03:30	22110	
sara031	Sara 0.9m	Jun 3	4:15:00	26100:30	CCD
sjk-0404	Hawaii UH 0.6m	Jun 3	5:59:30	31270	
jsx-0105	BAO 0.85m	Jun 3	13:27:50	4185	
sjk-0405	Hawaii UH 0.6m	Jun 3	14:42:30	1465	
jsx-0106	BAO 0.85m	Jun 3	16:00:20	8725	
suh-095	Suhora 0.6m	Jun 3	20:02:50	19055	
jr0603	Moletai 1.65m	Jun 3	20:24:55	12305	
sa-od037	SAAO 0.75m	Jun 3	20:49:00	10655	
teide17	Tenerife IAC 0.8m	Jun 4	00:26:00	16760	
sara032	Sara 0.9m	Jun 4	4:08:00	26940	CCD
sjk-0406	Hawaii UH 0.6m	Jun 4	5:37:00	34055	
tsm-0083	McDonald 2.1m	Jun 4	7:46:30	11310	
jsx-0107	BAO 0.85m	Jun 4	12:32:50	25280	
suh-096	Suhora 0.6m	Jun 4	20:21:00	16775	
sa-od039	SAAO 0.75m	Jun 4	21:42:00	7110	
calto0604	Calar Alto 1.23m	Jun 4	23:06:37	4290	CCD
teide19	Tenerife IAC 0.8m	Jun 5	0:14:30	17270	
tsm-0084	McDonald 2.1m	Jun 5	3:00:00	6150	
sara034	Sara 0.9m	Jun 5	4:47:00	24720	CCD
jsx-0108	BAO 0.85m	Jun 5	12:33:20	25295	
suh-097	Suhora 0.6m	Jun 5	20:04:00	18545	
jr0605_1	Moletai 1.65m	Jun 5	20:58:25	5555	
sa-od042	SAAO 0.75m	Jun 5	21:49:00	8005	
jr0605_2	Moletai 1.65m	Jun 5	22:52:55	3925	
teide20	Tenerife IAC 0.8m	Jun 6	1:08:00	13685	
tsm-0085	McDonald 2.1m	Jun 6	2:55:00	28800	
sara035	Sara 0.9m	Jun 6	4:08:00	10080	CCD
edjoh01	NOT	Jun 6	21:33:40	10150	
edjoh02	NOT	Jun 7	1:33:10	13025	
teide22	Tenerife IAC 0.8m	Jun 7	0:16:40	16850	
teide23	Tenerife IAC 0.8m	Jun 7	21:00:00	28800	
edjoh03	NOT 2.5m	Jun 7	22:23:40	15755	
suh-098	Suhora 0.6m	Jun 8	20:05:10	17065	
sara036	Sara 0.9m	Jun 10	4:41:00	7800	CCD
sara037	Sara 0.9m	Jun 11	4:01:00	9780	CCD
sara038	Sara 0.9m	Jun 12	3:57:00	10600	CCD
sara039	Sara 0.9m	Jun 20	7:09:00	14700	CCD
sara040	Sara 0.9m	Jun 21	3:36:00	28920	CCD
sara041	Sara 0.9m	Jun 22	3:29:00	22020	CCD
sara042	Sara 0.9m	Jun 23	3:23:00	28680	CCD

pulsation at this time. The other two lightcurves, however, each containing several pulsation modes, are less sinusoidal. If the non-sinusoidal nature of a lightcurve comes from the fact that many modes are present simultaneously, then one would expect the shape of the lightcurve to be sinusoidal only when it is pulsating in a single mode. On the other hand, in the August 1996 sinusoidal lightcurve, the peak-to-peak light variation was about 44% of the star's average light in the optical. We would expect such a large light variation to introduce nonlinear effects into the lightcurve, even if the star is pulsating in a single mode, causing the lightcurve to look nonsinusoidal. Thus, the nearly sinusoidal shape of our lightcurves (Fig. 8) is a mystery, except for the theoretical models of Ising & Koester 2001, which predict sinusoidal shapes for large amplitude modes even with the nonlinear response of the envelope.

After the $P = 423$ s mode reached its highest amplitude in run an-0034, the $k = 9$ $P = 464$ s mode started to grow and the 423 s became smaller, but there was still very little sign of the usually dominant $k = 17$ $P = 770$ s mode. In Fig. 2, we present the Fourier amplitude spectra of the light curves obtained each year, 2000 on top, 1996, 1994, and 1900 on the bottom, on the same vertical scale. Note that the 1996 data set is low resolution, because of its smaller amount of data. It is clear that the periodicities change amplitude from one data set to the other. It is important to

Telescope	Run	Date (UT)	Time(UT)	Length (s)
PdM 2m	gv-0480	1996 Sep 10	20:29:01	5670
Suhora 60cm	suh-62	1996 Sep 11	18:11:00	10790
PdM 2m	gv-0484	1996 Sep 14	21:22:02	2330
Suhora 60cm	suh-63	1996 Sep 18	18:45:00	15860
Suhora 60cm	suh-65	1996 Sep 19	18:06:20	13380
McD 2.1m	an-0061	1997 Apr 1	06:54:20	415
McD 2.1m	an-0066	1997 Apr 7	06:52:50	1763

Table 4. Journal of Observation for September, 1996 and April, 1997. September, 1996 data were taken by our Whole Earth Telescope collaborators during a WET run whose primary target was not GD 358. PdM stands for Pic du Midi in France, and Suhora is for Mt. Suhora in Poland. The 1997 data were all taken at McDonald Observatory in Texas.

notice that the periodicities, when present, have similar frequencies over the years. The amplitudes change, and even subcomponents (different m values) may appear and disappear, but when they are present, they have basically the same frequencies (typically to within $1 \mu\text{Hz}$).

In the September 1996 data, the Fourier transform shows that GD 358 is pulsating in periods similar to what we are familiar with from the WET data of 1990, although the highest peaks are at $1082 \mu\text{Hz}$, $2175 \mu\text{Hz}$ and $2391 \mu\text{Hz}$. The very limited data set and the complex pulsating structure of the star makes interpretation of these peaks difficult (Fig. 7). It is not until the data taken in April 1997 when we observe the 770 s mode as the highest amplitude mode in the Fourier transform, as in 1990 and 1994. We do not have data to fill in the gap between September 1996 and April 1997 to see how the amplitude changed, but even by August 19th, the modes at $k = 15$ and 18 were already starting to appear. The time scale which the star took to change from its normal multi-mode state to a single mode pulsator was very short, about one day. The reverse transition started one week after the event. An estimate of the total energy observed in pulsations is best obtained by measuring the peak-to-peak amplitudes in the light curves directly, instead of adding the total power from all the modes. For the largest amplitude run in 1996, an-0034, observed with the 82" telescope at McDonald, we estimate a peak-to-peak semi-amplitude of 220 mma. For comparison, the measured Fourier amplitude for the $k = 8$ mode for that run is 170 mma. For two runs at the same telescope in 2000, we obtain a peak-to-peak semi-amplitude of 120 mma. Again for comparison, the Fourier amplitudes of the large modes present are 30 mma, but there are several modes, and many combination peaks. As the observed pulsation energy is quadratic in the amplitudes and the frequencies, it corresponds to an increase of around 34% in the radiated energy by pulsations, from the amplitudes, plus a factor of 2.8 from the frequency. Just two days after the “forte”, the peak-to-peak amplitude decreased by a factor of 5, but during our observations a month later, it had already increased to its pre-“forte” value. It is important to notice that the observed amplitude is not directly a measurement of the physical amplitude, as there are several factors that typically depend on ℓ , including: geometrical cancellation, inclination effects, kinetic energies associated with the oscillatory mass motions, together with a term that depends on the frequency of pulsation squared. If we assume that the inclination angle of the pulsation axis to our line of sight does not change, and that the ℓ values of the dominant modes do not change, then it must be the ℓ distribution of the combination frequencies that changes and produces a difference in the peak-to-peak variations in the light curve, *if the total energy is conserved*. This is plausible, as relatively small variations in the amplitudes of the dominant periods can dramatically change the amplitudes of the linear combination frequencies, but not necessary.

4. Main Periodicities in the 2000 WET Data

4.1. Assumptions and Ground Rules Used in this Work

We observed GD 358 as the primary target in May-June of 2000 to provide another “snapshot” of the behavior of GD 358 with minimal alias problems. For the period May 23rd to June 8th, this run provided coverage ($\sim 80\%$) that was intermediate between the 1994 run (86% coverage) and the 1990 run (with 69% coverage). The 2000 WET run had several objectives: 1) look for additional modes besides the known $\ell = 1$ $k = 8$ through 18 modes; 2) investigate the multiplet splitting structure of the pulsation modes; 3) look for amplitude changes of the known modes; 4) determine the structure of the “combination peaks”, including the maximum order seen; and 5) provide simultaneous observations for HST time resolved spectroscopy.

Before we can start interpreting the peaks in the FT, we need to select an amplitude limit for what constitutes a “real” peak versus a “noise” peak. Kepler (1993) and Schwarzenberg-Czerny (1991, 1999), following Scargle (1982), demonstrated that non-equally spaced data sets and multiperiodic light curves, as all the Whole Earth Telescope data sets are, do not have a normal noise distribution, because the residuals are correlated. The probability that a peak in

Table 5. Average amplitude of datasets, from 1000 to 3000 μHz .

Year	BCT _{start} (days)	$\langle\text{Amp}\rangle$ (mma)
1990	244 8031.771867	0.62
1994	244 9475.001705	0.58
1996	245 0307.617884	1.44
2000	245 1702.402508	0.29

the Fourier transform has a 1/1000 chance of being due to noise, not a real signal, for our large frequency range of interest,¹ requires at least peaks above $4\langle\text{Amp}\rangle$, where the average amplitude $\langle\text{Amp}\rangle$ is the square root of the power average (see also Breger et al. 1993 and Kuschnig et al. 1997 for a similar estimative).

Table 5 shows that the noise, represented by $\langle\text{Amp}\rangle$, for the 2000 data set is the smallest to date, allowing us to detect smaller amplitude peaks. Several peaks in the multi-frequency fits are below the $4\langle\text{Amp}\rangle$ limit and therefore should be considered only as upper limits to the components.

The present mode identification follows that of the 1990 data set, published by Winget et al. (1994). They represent the pulsations in terms of spherical harmonics $Y_{\ell,m}$, with each eigenmode described by three quantum numbers: the radial overtone number k , the degree ℓ , also called the angular momentum quantum number, and the azimuthal number m , with $2\ell + 1$ possible values, from $-\ell$ to $+\ell$. For a perfectly spherical star, all $(2\ell + 1)$ eigenmodes with the same values of k and ℓ should have the same frequency, but rotation causes each eigenmode to have a frequency also dependent on m . Magnetic fields also lift the m degeneracy. The assigned radial order k value are the outcome of a comparison with model calculations presented in Bradley & Winget (1994), and are consistent with the observed mass and parallax, as discussed in their paper. Vuille et al. (2000) determinations followed the above ones. In the upper part of Fig.(1), we placed a mark for equally spaced periods (correct in the asymptotic limit), using the 38.9 s spacing derived by Vuille et al., starting with the $k = 17$ mode. The observed period spacings in the FT are very close to equal, consistent with previous observations.

4.2. Nonlinear Least Squares Results from 1990, 1994, and 1996

For a more self-consistent comparison, we took the data from the 1990, 1994 WET runs and the August 1996 run and derived the periods of the dominant modes via a nonlinear least squares fit. In Tables 6, 7 and 8 we present the results of a non-linear simultaneous least squares fit of 23 to 29 sinusoids, representing the main periodicities, to the 1990, 1994 and 1996 data sets. We use the nomenclature k^a , for example 15^- , to represent a subcomponent with $m = -1$ of the $k = 15$ mode in these tables. The difference in the frequencies reported in this paper compared to the previous ones is due to our use of the simultaneous non-linear least-squares frequency fitting rather than using the Fourier Transform frequencies.

We note that both the Fourier analysis and multi-sinusoidal fit assume the signal is composed of sinusoids with constant amplitudes, which is clearly violated in the 1996 data set. The changing amplitudes introduce spurious peaks in the Fourier transform. This will not affect the frequency of the modes, but the inferred amplitude will be a poor match to the (non-sinusoidal) light curve amplitude.

In Table 5 we present the average amplitude of the data sets, from 1000 to 3000 μHz , after the main periodicities, all above $4\langle\text{Amp}\rangle$, have been subtracted. For the 2000 data set, the initial $\langle\text{Amp}\rangle$ for the frequency range from 0 to 10 000 μHz , is 0.69 mma. For the high frequency range above 3000 μHz , $\langle\text{Amp}\rangle \simeq 0.2$ mma.

4.3. Mode Analysis of the 2000 WET Data

To provide the most accurate frequencies possible, we rely on a non-linear least squares fit of sinusoidal modes with guesses to the observed periods, since these better take into account contamination or slight frequency shifts due to aliasing. In Table 9 we present the results of a simultaneous non-linear least squares fit of 29 sinusoids, representing the main periodicities of the 2000 data set, simultaneously. All the phases have been measured with respect to the barycentric Julian coordinated date BCT 2 451 702.402 508.

Armed with the new frequencies in Table 9, we comment on regions of particular interest in the FT. First, we identify several newly detected modes at $P = 373.76$ s, $f = 2675.49$ μHz , amp=8.43 mma; $P = 852.52$ s, $f = 1172.99$ μHz , amp=2.74 mma; and $P = 900.13$ s, $f = 1110.95$ μHz , amp=2.03 mma. Based on the mode assignments of Bradley & Winget (1994) we identify these modes as $k = 7, 19,$ and 20 . The mode identification is based on the proximity of

¹ corresponding to a number of multiple trials larger than the number of data points

Table 6. Our multisinusoidal fit to the main periodicities in 1990.

k	Frequency (μHz)	Amplitude (mma)	T_{max} (s)
18	1233.408 ± 0.017	5.05 ± 0.13	731 ± 7
17 ⁺	1291.282 ± 0.018	5.04 ± 0.14	395 ± 6
17	1297.590 ± 0.006	14.60 ± 0.14	24 ± 2
17 ⁻	1303.994 ± 0.019	4.71 ± 0.14	411 ± 7
16 ⁺	1355.664 ± 0.106	0.87 ± 0.14	471 ± 37
16	1361.709 ± 0.040	2.21 ± 0.14	18 ± 14
16 ⁻	1368.568 ± 0.031	2.96 ± 0.14	627 ± 11
15 ⁺	1420.932 ± 0.010	9.32 ± 0.14	416 ± 3
15	1427.402 ± 0.005	19.24 ± 0.14	425 ± 2
15 ⁻	1433.853 ± 0.011	7.90 ± 0.14	88 ± 4
14 ⁺	1513.023 ± 0.017	5.23 ± 0.14	123 ± 5
14	1518.991 ± 0.009	9.71 ± 0.14	270 ± 3
14 ⁻	1525.873 ± 0.016	5.35 ± 0.13	459 ± 5
13 ⁺	1611.671 ± 0.016	5.70 ± 0.14	140 ± 5
13	1617.297 ± 0.017	5.28 ± 0.14	508 ± 5
13 ⁻	1623.644 ± 0.019	4.70 ± 0.14	407 ± 5
12	1733.850 ± 0.163	0.53 ± 0.13	474 ± 44
11 ⁺	1840.022 ± 0.136	0.65 ± 0.14	41 ± 35
11	1846.247 ± 0.135	0.66 ± 0.14	504 ± 34
11 ⁻	1852.099 ± 0.093	0.94 ± 0.14	132 ± 24
10 ⁺	1994.240 ± 1.071	≤ 0.14	
10	1998.919 ± 0.060	1.50 ± 0.14	25 ± 14
10 ⁻	2007.992 ± 0.117	0.84 ± 0.14	7 ± 26
9 ⁺	2150.430 ± 0.048	1.932 ± 0.13	174 ± 10
9	2154.052 ± 0.020	4.59 ± 0.13	336 ± 4
9 ⁻	2157.834 ± 0.032	2.81 ± 0.13	400 ± 7
8 ⁺	2358.975 ± 0.016	5.68 ± 0.13	120 ± 3
8	2362.588 ± 0.016	5.77 ± 0.13	422 ± 3
8 ⁻	2366.418 ± 0.017	5.34 ± 0.13	268 ± 3

the detected modes with those predicted by the models, or even the asymptotical period spacings, but also because of resonant mode coupling, i.e., a stable mode will be driven to visibility if a coupled mode falls near its frequency, as it happens for $k = 7$, which is very close to the combination of $k = 17$ and $k = 16$, and $k = 20$, which falls near the resonance of the 8^- and the $\ell = 2$ mode at $1255 \mu\text{Hz}$ (see next paragraph). It is important to note that these modes appear in combination peaks with other modes, as shown in Table 11. This reinforces our belief that these modes are physical modes, and not just erroneously identified combination peaks. We note that Bradley (2002) analyzed single site data taken over several years, and found peaks at 1172 or $1183 \mu\text{Hz}$ in April 1985, May 1986, and June 1992 data, lending additional credence to the detection of the $k = 19$ mode or its alias.

The first previously known region of interest surrounds the $k = 18$ mode, which lies near $1233 \mu\text{Hz}$, according to previous observations. In the 2000 data, the largest amplitude peak in this region lies at $1255 \mu\text{Hz}$, which is over $20 \mu\text{Hz}$ from the previous location. Given that other modes (especially the one at $k = 17$) has shifted by less than $4 \mu\text{Hz}$, we are inclined to rule out the possibility that the $k = 18$ mode shifted by $20 \mu\text{Hz}$. One possible solution is offered by seismological models of GD 358, which predict an $\ell = 2$ mode near $1255 \mu\text{Hz}$. For example, the best ML2 fit to the 1990 data (from Metcalfe, Salaris & Winget 2002, Table 3), has an $\ell = 2$ mode at $1252.6 \mu\text{Hz}$ ($P=798.3$ s). This would also be consistent with the larger number of subcomponents detected, although they may be caused only by amplitude changes during the observations. Fig (9) shows the region of the $k = 18$ mode in the FT for the 1990 data set (solid) and the 2000 data set (dashed); it is consistent with the $k = 18$ mode being the $1233 \mu\text{Hz}$ for both data sets, and they even have similar amplitudes. While we avoided having to provide an explanation for why only the $k = 18$ mode would shift by $20 \mu\text{Hz}$, we have introduced another problem, as geometrical cancellation for an $\ell = 2$ mode introduces a factor of 0.26 in relation to unity for an $\ell = 1$ mode. Thus, the identification of the $1255 \mu\text{Hz}$ as an $\ell = 2$ mode, which has a measured amplitude of 14.86 mma , implies a physical amplitude higher than that of the highest amplitude $\ell = 1$ mode, around 30 mma .

Kotak et al. (2002), analyzing time-resolved spectra obtained at the Keck in 1998, show the velocity variations of the $k = 18$ mode at $1233 \mu\text{Hz}$ is similar to those for the $k = 15$ and $k = 17$ modes, concluding all modes are $\ell = 1$. They did not detect a mode at $1255 \mu\text{Hz}$.

Table 7. Main periodicities in 1994.

k	Frequency (μHz)	Amplitude (mma)	T_{max} (s)
18 ⁺	1228.712 \pm 0.022	2.77 \pm 0.13	252.6 \pm 12.0
18	1235.493 \pm 0.005	12.94 \pm 0.13	170.9 \pm 2.6
18 ⁻	1242.364 \pm 0.016	3.66 \pm 0.13	62.4 \pm 9.0
17 ⁺	1291.093 \pm 0.010	6.17 \pm 0.13	250.3 \pm 5.1
17	1297.741 \pm 0.003	22.11 \pm 0.13	37.7 \pm 1.4
17 ⁻	1304.459 \pm 0.010	6.25 \pm 0.13	615.0 \pm 5.0
16 ⁺	1355.388 \pm 0.035	1.70 \pm 0.13	167.0 \pm 17.6
16	1362.298 \pm 0.060	< 0.89	
16 ⁻	1368.541 \pm 0.031	1.92 \pm 0.13	322.3 \pm 15.5
15 ⁺	1419.650 \pm 0.003	18.37 \pm 0.13	46.4 \pm 1.6
15	1426.408 \pm 0.004	15.55 \pm 0.13	239.7 \pm 1.8
15 ^a	1430.879 \pm 0.006	10.61 \pm 0.13	187.9 \pm 2.7
15 ⁻	1433.169 \pm 0.014	4.46 \pm 0.13	104.1 \pm 6.5
14	1519.903 \pm 0.028	1.09 \pm 0.13	485.2 \pm 20.0
13 ⁺	1611.357 \pm 0.012	5.02 \pm 0.13	466.0 \pm 5.0
13	1617.474 \pm 0.009	3.46 \pm 0.13	183.3 \pm 1.1
13 ⁻	1624.568 \pm 0.010	6.07 \pm 0.13	101.0 \pm 4.1
12	1746.766 \pm 0.064	0.93 \pm 0.13	414.2 \pm 25.0
11	1863.004 \pm 0.184	< 0.71	
10	2027.325 \pm 0.457	< 0.46	
9 ⁺	2150.504 \pm 0.019	3.15 \pm 0.13	346.7 \pm 6.1
9	2154.124 \pm 0.013	4.76 \pm 0.13	12.3 \pm 4.0
9 ⁻	2157.841 \pm 0.022	2.69 \pm 0.13	144.2 \pm 7.1
8 ⁺	2358.883 \pm 0.013	4.50 \pm 0.13	398.2 \pm 3.8
8	2362.636 \pm 0.006	9.25 \pm 0.13	274.6 \pm 1.8
8 ⁻	2366.508 \pm 0.007	4.22 \pm 0.13	169.7 \pm 3.8

In Fig. 10 we show the pre-whitened results; pre-whitening was done by subtracting from the observed light curve a synthetic light curve constructed with a single sinusoid with frequency, amplitude and phase that minimizes the Fourier spectrum at the frequency of the highest peak. A new Fourier spectrum is calculated and the next dominant frequency is subtracted, repeating the procedure until no significant power is left. It is important to notice that with pre-whitening, the order of subtraction matters. As an example, in the 2000 data set, if we subtract the largest peak in the region of the $k = 18$ mode, at 1255.41 μHz , followed by the next highest peak at 1256.26 μHz and the next at 1254.44 μHz , we are left with a peak at only 1.3 mma at 1232.76 μHz . But if instead we subtract only the 1255.41 μHz followed by the peak left at 1233.24 μHz , its amplitude is around 3.1 mma, i.e., larger. Pre-whitening assumes the frequencies are independent in the observed, finite, data set. If they were, the order of subtraction would not affect the result. Because the order of subtraction matters, the basic assumption of pre-whitening does not apply. We attempt to minimize this effect by noting that the frequencies change less than the amplitudes, and use the FT frequencies in a simultaneous non-linear least squares fit of all the eigenmode frequencies. But even the simultaneous non-linear least squares fit uses the values of the Fourier transform as starting points, and could converge to a local minimum of the variance instead of the global minimum.

The modes with periods between 770 and 518 s ($k = 17$ through 13) are present in the 2000 data, though with different amplitudes than in previous years. Another striking feature of the peaks in 2000 is that one multiplet member of each mode has by far the largest amplitude, so that without data from previous WET runs, we would not know that the modes are rotationally split. The frequencies of these modes are stable to about 1 μHz or less with the exception of the 16⁻ mode, where the frequency jumped from about 1368.5 μHz in 1990 and 1994 to about 1379 μHz in 1996 and 2000 (see Fig. 11). Most of these frequency changes are larger than the formal frequency uncertainty from a given run (typically less than 0.05 μHz), so there is some process in GD 358 that causes the mode frequencies to “wobble” from one run to the next. We speculate that this may be related to non-linear mode coupling effects. Whatever the origin of the frequency shifts, it renders these modes useless for studying evolutionary timescales through rates of period change.

The $k = 12$ through 10 modes deserve separate mention because their amplitudes are always small; between 1990 and 2000, the largest amplitude peak was only 1.6 mma. The small amplitudes can make accurate frequency determinations difficult, and all three modes have frequency shifts of 13 to 33 μHz between the largest amplitude peaks in a given mode. The $k = 10$ mode shows the largest change with the 1990 data showing the largest peaks at

Table 8. Main modes in 1996.

k	Frequency (μHz)	Amplitude (mma)	T_{max} (s)
19	1172.66 ± 0.15	2.5 ± 0.6	17.4 ± 47.5
18	1253.65 ± 1.01	< 2.1	
17 ⁺	1291.13 ± 0.11	4.3 ± 0.6	653.6 ± 28.1
17 ⁰	1295.38 ± 0.17	2.6 ± 0.6	139.7 ± 43.6
17 ⁻	1304.68 ± 0.11	4.8 ± 0.6	346.3 ± 25.7
16 ⁺	1355.21 ± 2.02	< 1.9	
16 ⁰	1362.55 ± 0.15	2.7 ± 0.6	172.2 ± 41.2
16 ⁻	1379.64 ± 0.16	2.7 ± 0.6	378.6 ± 41.0
15 ⁰	1427.47 ± 0.92	< 2.2	
15 ⁻	1434.36 ± 0.18	2.2 ± 0.6	154.5 ± 47.1
14	1520.58 ± 0.18	2.0 ± 0.6	398.3 ± 46.6
13 ⁺	1611.60 ± 0.18	2.1 ± 0.6	461.8 ± 42.7
13 ⁰	1617.51 ± 0.35	1.1 ± 0.6	183.5 ± 79.9
13 ⁻	1619.63 ± 0.84	< 2.2	
12	1736.10 ± 0.34	1.1 ± 0.6	323.6 ± 75.2
11	1862.93 ± 0.39	0.9 ± 0.6	58.8 ± 78.7
10	2027.41 ± 0.26	1.4 ± 0.6	471.9 ± 47.9
9 ⁺	2149.97 ± 0.07	5.6 ± 0.6	69.8 ± 11.8
9 ⁰	2153.84 ± 0.05	7.6 ± 0.6	155.2 ± 8.5
9 ⁻	2157.89 ± 0.04	9.1 ± 0.6	426.7 ± 7.2
8 ⁺	2358.63 ± 0.03	12.6 ± 0.6	125.3 ± 4.7
8 ⁰	2362.50 ± 0.02	23.2 ± 0.6	104.8 ± 2.5
8 ⁻	2365.98 ± 0.02	22.2 ± 0.6	142.9 ± 2.6

Table 9. Main modes in 2000.

k	Frequency (μHz)	Period (sec)	Amplitude (mma)	T_{max} (s)
20	1110.960 ± 0.017	900.122 ± 0.014	2.04 ± 0.08	870.19 ± 8.61
19	1172.982 ± 0.013	852.528 ± 0.009	2.74 ± 0.08	164.86 ± 6.07
$\ell = 2$	1255.400 ± 0.002	796.556 ± 0.002	14.86 ± 0.08	747.02 ± 1.05
18	1233.595 ± 0.018	810.639 ± 0.012	1.96 ± 0.08	354.91 ± 8.11
17 ⁺	1294.284 ± 0.094	772.628 ± 0.056	0.38 ± 0.082	579.63 ± 39.54
17	1296.599 ± 0.001	771.248 ± 0.001	29.16 ± 0.08	247.81 ± 0.52
17 ⁻	1301.653 ± 0.053	768.254 ± 0.031	0.68 ± 0.08	314.52 ± 22.52
16	1362.238 ± 0.159	734.086 ± 0.086	0.42 ± 0.12	263.36 ± 63.93
16 ⁻	1378.806 ± 0.007	725.265 ± 0.004	5.35 ± 0.08	514.70 ± 2.66
15 ⁺	1420.095 ± 0.001	704.178 ± 0.001	29.69 ± 0.08	418.14 ± 0.49
15	1428.090 ± 0.052	700.236 ± 0.025	0.70 ± 0.08	217.29 ± 19.78
15 ⁻	1432.211 ± 0.036	698.221 ± 0.018	1.08 ± 0.089	355.58 ± 13.30
14	1519.811 ± 0.134	657.977 ± 0.058	0.266 ± 0.08	301.55 ± 48.28
13 ⁺	1611.084 ± 0.116	620.700 ± 0.045	0.31 ± 0.08	448.66 ± 39.81
13	1617.633 ± 0.174	618.187 ± 0.066	0.21 ± 0.08	448.19 ± 58.97
13 ⁻	1625.170 ± 0.235	615.320 ± 0.089	0.15 ± 0.08	299.24 ± 79.32
12	1736.277 ± 0.034	575.945 ± 0.011	1.04 ± 0.08	230.37 ± 10.79
11	1862.871 ± 0.042	536.806 ± 0.012	0.84 ± 0.08	503.66 ± 12.43
10	2027.008 ± 0.028	493.338 ± 0.007	1.29 ± 0.08	350.14 ± 7.49
9 ⁺	2150.462 ± 0.012	465.016 ± 0.003	2.96 ± 0.08	35.49 ± 3.09
9	2154.021 ± 0.007	464.248 ± 0.001	5.34 ± 0.08	252.38 ± 1.71
9 ⁻	2157.731 ± 0.014	463.450 ± 0.003	2.57 ± 0.08	174.68 ± 3.53
8 ⁺	2359.119 ± 0.006	423.887 ± 0.001	5.57 ± 0.08	166.60 ± 1.49
8	2362.948 ± 0.094	423.200 ± 0.017	0.38 ± 0.08	81.50 ± 21.93
8 ⁻	2366.266 ± 0.006	422.607 ± 0.001	5.79 ± 0.08	418.36 ± 1.44
2×18	2510.761 ± 0.021	398.286 ± 0.003	1.70 ± 0.08	334.47 ± 4.58
2×17	2593.208 ± 0.004	385.623 ± 0.001	7.82 ± 0.08	249.57 ± 0.96
7	2675.487 ± 0.004	373.764 ± 0.001	8.49 ± 0.08	193.30 ± 0.86
2×15	2840.195 ± 0.008	352.089 ± 0.001	4.29 ± 0.08	47.50 ± 1.60

1998.7 μHz and 2008.2 μHz , while the 2000 data has one peak dominating the region at 2027.0 μHz . An examination of the data in Bradley (2002) shows that the $k = 12$ mode seems to consistently show a peak near 1733 to 1736 μHz , and that only the 1994 data has the peak shifted to 1746.8 μHz , suggesting that 1994 data may have found an alias peak or that the 1736 μHz mode could be the $m = +1$ member and the 1746.8 μHz mode is the $m = -1$ member. The data in Bradley (2002) do not show convincing evidence for the $k = 11$ or 10 modes, so we cannot say anything else about them.

It is interesting to note that the $k = 8$ and $k = 9$ modes are always seen as a triplet, with 3.58 μHz separation for $k = 9$, even in the 1996 data set. Our measured spacings are 3.54 and 3.69 μHz , from $m = -1$ to $m = 0$ and $m = 0$ to $m = 1$. The $k = 8$ mode in 2000 shows an $m=0$ component below our statistical detection limit ($A=0.41$ mma, when the local $\langle \text{Amp} \rangle = 0.29$ mma), but the $m = 1$ and $m = -1$ modes remain separated by 2×3.58 μHz . All the higher k modes are seen as singlets in the 2000 data set. We also note that the $k = 8$ and 9 modes have by far the most stable frequencies. The frequencies are always the same to within 0.3 μHz , and in some cases better than 0.1 μHz . However, the frequency shifts are large enough to mask any possible signs of evolutionary period change, as Fig. 12 shows. Thus, we are forced to conclude that GD 358 is not a stable enough “clock” to discern evolutionary rates of period change.

5. Multiplet Splittings

As pointed out by Winget et al. (1994) and Vuille et al. (2000), the observed triplets in the 1990 and 1994 data sets had splittings ranging from 6.5 μHz from the “external” modes (such as $k = 17$) to 3.6 μHz for the “internal” modes $k = 8$ and 9. Winget et al. interpreted these splittings to be the result of radial differential rotation, and Kawaler et al. (1999) examined this interpretation in more detail. An examination of the frequencies found in the 2000 data set, shown in Table 9, shows that the multiplet structure is much harder to discern, since the $k = 10$ through 20 modes typically have only one multiplet member with a large amplitude. The obvious multiplet members have frequencies that agree with the 1990 data, except for the 16^- mode, where there is a +10.234 μHz shift in the 2000 data.

Note that the $k = 10$ mode identified at 2027 μHz is different than the 1994 μHz identified by Winget et al. (1994) in the 1990 data. However, the peak they identified is not the highest peak in that region of the Fourier transform (see Fig. 13). Our analysis of the 1990 data has statistically significant $k = 10$ peaks close to 1999 μHz and 2008 μHz .

The only modes with obvious multiplet structure are the $k = 9$ mode, which still shows an obvious 3.6 μHz split triplet, and the $k = 8$ mode, which shows two peaks that are consistent with 2×3.6 μHz separation.

In Table 11 we have a peak 3.3 μHz from the $k = 15$, $m = 1$ mode that we have not seen before; we call it the 15^b mode. We are not certain whether this is another member of the $k = 15$ multiplet (analogous to the 15^a mode in the 1994 WET data) or if it is something else. The 1994 data set also presented a large peak 4.4 μHz from $k = 15$, $m = 0$, which we call the 15^a mode, in addition to the $m = \pm 1$ components. We have not seen this 15^a mode in any other data set other than the 1994 WET run. The identity of the “extra subcomponents” remains an unsolved mystery.

6. Linear Combinations

Winget et al. (1994) and Vuille et al. (2000) show that most of the periodicities are in fact linear combination peaks of the main peaks (eigenmodes). Combination peaks are what we call peaks in the FT whose frequencies are equal to the sum or difference of two (or more) the $\ell = 1$ or 2 mode frequencies. The criteria for selection of the combination peaks was that the frequency difference between the combination peak and the sum of the “parent mode” frequencies must be smaller than our resolution, which is typically around 1 μHz . The last column of Table 11 shows the frequency difference.

**** TABLE 11 - Linear combinations (should be here) ***

For example, only 28 of the more than 180 peaks in Winget et al. (1994) are $\ell = 1$ modes; the rest are combination peaks up to third order (i.e., three modes are involved). The $\ell = 1$ modes lie in the region 1000 to 2500 μHz , and are identified as modes $k = 18$ to 8. In the 1994 data set analyzed by Vuille et al., combination peaks up to 4th order were detected. In the 2000 data set we identify combination peaks up to 6th order, and most if not all remaining peaks are in fact linear combination peaks, as demonstrated in Table 11 and is shown in the pre-whitened FT of the 2000 data (see Fig. 14). Here too, we use the nomenclature k^a , for example 15^- , to represent a subcomponent with $m = -1$ of the $k = 15$ mode.

The so-called $\ell = 2$ mode at 1255 μHz , as well as $k = 17$ and $k = 15$ modes, have subcomponents, but probably they are not different m value components, and are caused, most likely, by amplitude modulation. We say this because the frequency splittings are drastically different than in previous data, and for the $\ell = 2$ mode, there are more than 5 possible subcomponent peaks present. We did not do an exhaustive search for all of the possible combination peaks up to 6th order in the Fourier transform, as we only took into account the peaks that had a probability smaller than 1/1000 of being due to noise, and studied if they could be explained as combination peaks.

Table 10. Optimal Fits to 2000 data.

Parameter	Fit <i>a</i>	Fit <i>b</i>	Fit <i>c</i>	Fit <i>d</i>
$T_{\text{eff}} (K)$	24,300	23,500	24,500	22,700
$M_* (M_{\odot})$	0.61	0.60	0.625	0.630
$\log(M_{\text{He}}/M_*)$	-2.79	-5.13	-2.58	-4.07
X_{O}	0.81	0.99	0.39	0.37
$q(m/M_*)$	0.47	0.47	0.83	0.42
$\sigma_P (s)$	2.60	3.65	2.12	1.72
$\sigma_{\Delta P} (s)$	4.07	4.92	2.21	...

Brickhill’s (1992) pulsation–convection interaction model predicts, and the observations reported by Winget et al. and Vuille et al. agree, that a combination peak involving two different modes always has a larger relative amplitude than a combination involving twice the frequency of a given mode (also called a harmonic peak). Wu’s (2001) analytical expression leads to a factor of 1/2 difference between a combination peak with two modes versus a harmonic peak, assuming that the amplitudes of both eigenmodes are the same. Vuille et al. claim that the relatively small amplitude of the $k = 13$ mode in 1994 is affected by destructive beating of the nonlinear peak ($2 \times 15 - 18$) and that the $k = 16$ mode amplitude is affected by the ($15 + 18 - 17$) combination peak. It is noteworthy that the peak at $1423.62 \mu\text{Hz}$ is only $3.52 \mu\text{Hz}$ from $k = 15$, so it might be the 15^- mode. However, the previously identified 15^- was $6.7 \mu\text{Hz}$ from it, and we consider the $1423.62 \mu\text{Hz}$ peak to be either a result of amplitude modulation of the $k = 15$ mode or yet another combination peak.

We note that the wealth of combination peaks and their relative amplitude offers insight into the amplitude limiting mechanism and would be worthy of the considerable theoretical and numerical effort required to understand it.

7. Model-Fitting with a Genetic Algorithm

One of the major goals of our observations of GD 358 was to discover additional modes to help refine our seismological model fits. We were also interested in how much the globally optimal model parameters would change due to the slight shifts in the observed periods. With these goals in mind, we repeated the global model-fitting procedure of Metcalfe, Winget & Charbonneau (2001) on several subsets of the new observations.

Our model-fitting method uses the parallel genetic algorithm described by *** Metcalfe & Charbonneau (2002) to minimize the root-mean-square (rms) differences between the observed and calculated periods (P_k) and period spacings ($\Delta P \equiv P_{k+1} - P_k$) for models with effective temperatures (T_{eff}) between 20,000 and 30,000 K, total stellar masses (M_*) between 0.45 and 0.95 M_{\odot} , helium layer masses with $-\log(M_{\text{He}}/M_*)$ between 2.0 and ~ 7.0 , and an internal C/O profile with a constant oxygen mass fraction (X_{O}) out to some fractional mass (q) where it then decreases linearly in mass to zero oxygen at 0.95 m/M_* . This technique has been shown to find the globally optimal set of parameters consistently among the many possible combinations in the search space, but it requires between ~ 200 and 4000 times fewer model evaluations than an exhaustive search of the parameter-space to accomplish this, and has a failure rate $< 10^{-5}$.

We attempted to fit the 13 periods and period spacings defined by the $m = 0$ components of the 14 modes identified as $k = 7$ to $k = 20$ in Table 9. Because of our uncertainty about the proper identification of $k = 18$ (see section 4) we performed fits under two different assumptions: for Fit *a* we assumed that the frequency near $1233 \mu\text{Hz}$ was $k = 18$ (similar to the frequency identified in 1990), and for Fit *b* we assumed that the larger amplitude frequency near $1255 \mu\text{Hz}$ was $k = 18$. The results of these two fits led us to prefer the identification for $k = 18$ in Fit *a*, and we included this in an additional fit using only the 11 modes from $k = 8$ to $k = 18$, which correspond to those identified in 1990 (Fit *c*). We performed an additional fit (Fit *d*) that included the same 13 periods used for Fit *a*, but ignored the period spacings. The optimal values for the five model parameters, and the root-mean-square residuals between the observed and computed periods (σ_P) and period spacings ($\sigma_{\Delta P}$) for the four fits are shown in Table 10.

Our preferred solution from Table 10 is Fit *a*, because it includes our favored identification for the $k = 18$ mode and the additional pulsation periods. The larger $\sigma_{\Delta P}$ in Fit *a* compared to Fit *c* is dominated by the large period spacings between the $k = 19$ and 20 modes (47.6 s) and the $k = 7$ and 8 modes (49.4 s). Fit *a* has a mass and effective temperature that are essentially the same as the fit of Bradley & Winget (1994), and are consistent with the spectroscopic values derived by Beauchamp et al. (1999). The other structural parameters are otherwise similar to those found by Metcalfe et al. (2001) ($T_{\text{eff}} = 22,600$ K, $M_* = 0.650 M_{\odot}$, $\log(M_{\text{He}}/M_*) = -2.74$, $X_{\text{O}} = 0.84$, and $q = 0.49$). We caution, however, that the large values of σ_P and $\sigma_{\Delta P}$ for Fit *a* imply that our model may not be an adequate representation of the real white dwarf star. New and unmodeled physical circumstances may have arisen between 1994 and 2000 (e.g. whatever caused the *forte* in 1996), which may account for the diminished capacity of our simple model to match the observed periods.

8. Summary of Observational Clues

Before embarking on our discussion, we recap the highlights of our observations. First, the 2000 WET data shows eigenmodes from at least $k = 8$ through $k = 19$. We may also have detected the $k = 7$ and $k = 20$ modes. However, their frequencies are similar to that of unrelated combination peaks, so their identification is less secure. For the first time, we have also found an $\ell = 2$ mode in the GD 358 data; it is at $1255.4 \mu\text{Hz}$. Second, we see relatively few multiplet modes for a given k , with the exception of the $k = 8$ and 9 modes. While the multiplet structure of the $\ell = 1$ modes is muted, the combination peaks are enhanced to the point that we see combination modes up to 6th order. Combined with the previous WET runs, we see evidence for anticorrelation between the presence of multiplet structure and combination peaks. The presence of amplitude variability of the $\ell = 1$ mode continues. In the August 1996 data, we saw the most extreme example yet, where all of the observed light was in a single ($k = 8$ mode) for one night (which we call the “forte”). Data before and after the run show power in the nights before and after in other pulsation modes besides the $k = 8$ and a much lower amplitude. The periods from the 1996 data are consistent with the 2000 data set, although there are differences in the details.

9. Discussion and Puzzles

Using the $k = 7, 19$, and 20 modes in seismological fits produces a best-fitting model that is similar to that derived from only the $k = 8$ through 18 modes, indicating that the new modes do not deviate drastically from the expected mode pattern.

The reappearance of modes with frequencies similar to those obtained before the mode disappeared (true of all modes from $k = 8$ through 19), shows that the stellar structure sampled by these modes remained the same for almost 20 years. This is in spite of rapid amplitude change events like the “forte” one observed in August 1996. Our observations, coupled with guidance from the available theories of Brickhill (1992) and Wu & Goldreich (2001) suggest that the “forte” event was probably an extreme manifestation of a nonlinear mode-coupling event that did not materially affect the structure of the star other than possibly the driving region. The appearance and disappearance of modes is similar to the behavior observed in the ZZ Ceti star G 29-38 by Kleinman et al. (1998), and we note that “ensemble” seismology works for GD 358 as well as for the cool ZZ Ceti stars. The one caveat is that the $\sim 1 \mu\text{Hz}$ frequency “wobbles” will place a limit on the accuracy of the seismology.

We also appear to have discovered an $\ell = 2$ mode (at $1255.4 \mu\text{Hz}$) in GD 358 for the first time, based on the match of the observed period to that of $\ell = 2$ modes from our best fitting model. Our model indicates that this is the $k = 34$ mode. This mode has a relatively large amplitude of 14.9 mma , which combined with the increased geometric cancellation (about $3.8\times$) of an $\ell = 2$ mode, implies that it has the largest amplitude of any mode observed in 2000. We note the existence of several linear combination peaks involving the $1255 \mu\text{Hz}$ mode, that also show complex structures. This lends credence to the $1255 \mu\text{Hz}$ mode being a real mode, and that the complex structure is associated with the real mode (such as amplitude modulation), as opposed to being some sort of combination peak. The amplitude of the $1255 \mu\text{Hz}$ mode changed during the WET run, so we suspect that the many subcomponents observed are most likely due to amplitude modulation.

The period structure of the 1990 and 1994 WET data sets are similar, but show that the amplitude of the modes, and even the fine structure, changes with time. In August 1996, the period structure changed rapidly and dramatically, with essentially all the observed pulsation power going to the $k = 8$ mode. In spite of the large amplitude, the light curve was surprisingly sinusoidal, with a small contribution from the $k = 9$ mode. Single site observations one month earlier (June 1996) and one month later (September 1996) show a period structure similar to those present in the 1990 and 1994 data sets. For the 2000 data set, the period structure shows close to equal frequency splittings, and the fine structure is different than observed before. Only the $k = 9$ mode show the same clear triplet observed in 1990 and 1994, with the same frequency splitting. The $k = 8$ mode shows the $m = -1$ and $m = 1$ modes, while the central $m = 0$ mode is below our $4\langle\text{Amp}\rangle$ significance level. The other modes do not show clearly the triplet structure previously observed. The 1990 and 1994 data sets show the m-splitting expected by rotational splitting, but the change of the splitting frequency difference from $6 \mu\text{Hz}$ to $3 \mu\text{Hz}$ from $k = 17$ to $k = 8$ was interpreted as indicating differential rotation.

The apparent anticorrelation between the abundance of multiplet structure and the highest order of combination frequencies seen is a puzzle. As we do not expect the differential rotation profile of GD 358 changed in the last 10 years (and the splittings we do see in 2000 support this contention), the anticorrelation must be telling something about what is going on with rotation in the convection zone. We say this because the combination peaks are believed to be caused by the nonlinear response of the depth varying convection zone, and thus the increased order of combination peaks implies that the convection zone is more “efficient” at mixing eigenmodes to observable amplitudes. The $k = 8$ and 9 modes continue to show obvious multiplet structure and little, if any, change in splitting. These modes are the most “internal” of the observed modes of GD 358, and we speculate that this must have some bearing on their

multiplet structure’s ability to persist. We do not see any obvious pattern in the dominant amplitude multiplet member with overtone number, so there is not an obvious pattern of rotational coupling to the convection zone for determining mode amplitude. We will need theoretical guidance to make sense of these observations.

A related puzzle is the presence of extra multiplet members and/or apparent large frequency shifts of modes in the $k = 15$ and 16 multiplets. The $k = 15$ mode shows an extra component at $1430.88 \mu\text{Hz}$ in the 1994 data and a peak at $1423.62 \mu\text{Hz}$ in the 2000 data that have not been seen before or since. Some possible explanations include: rapid amplitude modulation of a $k = 15$ multiplet member that the FT interprets as an extra peak; the 2000 peak is about the right frequency to be another $\ell = 2$ mode, if we use the $1255.4 \mu\text{Hz}$ mode as a reference point; it could be an unattributed combination peak involving sums and differences of known modes; or it could be something else entirely. The large peak at about $1379 \mu\text{Hz}$ in 1996 and 2000 is also something of a mystery. It is possible that the $k = 16$, $m = -1$ component really changed by $10 \mu\text{Hz}$ from the $1368 \mu\text{Hz}$ observed in 1990, although we would have to explain why only this large amplitude multiplet member suffered this large a frequency change. Other possibilities include: the peak is a 1 cycle per day alias of another mode; the peak is a combination peak — the combination $15 + (\ell = 2) - 17$ is a perfect frequency match; or possibly an $\ell = 2$ mode, based on period spacing arguments. Further observations, data analysis with tools like wavelet analysis, and further model fitting may help determine which explanation fits the data best.

Brickhill (1992) proposed that the combination frequencies result from mixing of the eigenmode signals by a depth-varying surface convection zone when undergoing pulsation. He pointed out that the convective turnover time in DA and DB variable white dwarf stars occurs on a timescale much shorter than the pulsation period. As a consequence, the convective region adjusts almost instantaneously during a pulsation cycle. Brickhill demonstrated that the flux leaving the convective zone depends on the depth of the convective zone, which changes during the pulsation cycle, distorting the observed flux. This distortion introduces combination frequencies, even if the pulsation at the bottom of the convection zone is linear, i.e., a single sinusoidal frequency. Wu (2001) analytically calculated the amplitude and phases expected of such combination frequencies, and concluded that the convective induced distortion was roughly in agreement with GD358’s 1994 observations, provided that the inclination of the pulsation axis to the line of sight is between 40 deg and 50 deg . Wu also calculated that the harmonics for $\ell = 2$ modes should be much higher than for $\ell = 1$. However the theory overpredicts the amplitude of the $\ell = 1$ harmonics. She also predicts that geometrical cancellation will, in principle, allow a determination of ℓ if both frequencies sums and differences are observed. These predictions still need testing.

While Wu & Goldreich (2001) discuss parametric instability mechanisms for the amplitude of the pulsation modes, they only discuss the case where the parent mode is unstable and the daughter modes are stable. However, with GD 358, we have a different situation. The highest frequency $k = 8$ and 9 modes can have as a daughter mode one of the lower frequency ($k = 17, 18, \text{ or } 19$) $\ell = 1$ modes and an $\ell = \text{higher}$ mode. One or both of these daughter modes are actually pulsationally unstable as well, which we believe would require coupling to still lower frequency granddaughter modes that are predicted to be stable by our models and the calculations of Brickhill (1990, 1991) and Goldreich & Wu (1999a, b). We suggest that occasionally the nonlinear coupling of the granddaughter and daughter modes with the $k = 8$ and 9 modes can allow the $k = 8$ and 9 modes to suffer abrupt amplitude changes when everything is “just right”. In the meantime, the granddaughter modes will couple to the excited daughter modes ($k = 13$ through 19 in general) to produce the observed amplitude instability of these modes. We need a quantitative theoretical treatment of this circumstance worked out to see if the predicted behavior matches what we observe in GD 358.

Observations of GD 358 have been both rewarding and vexing. We have been rewarded with enough $\ell = 1$ modes being present to decipher the mode structure and perform increasingly refined asteroseismology of this star, starting with Bradley & Winget (1994) up to the latest paper of Metcalfe et al. (2002). One thing asteroseismology has not provided us with is the structure of and/or the depth of the surface convection zone. This would help us test the “convective driving” mechanism introduced by Brickhill (1991) and elaborated on by Goldreich & Wu (1999a,b). Our observations point out the need for further refinements of the parametric instability mechanism described by Wu & Goldreich (2001) to better cover the observed mode behavior. The observational data set is quite rich, and coupled with more detailed theories, offers the promise of being able to unravel the mysteries of amplitude variation seen in the DBV and DAV white dwarfs. This in turn, may offer us the insights needed to ascertain why only some of the predicted modes are seen at any one time.

MAW, AKJ, AEC, and MLB acknowledge support by the National Science Foundation through the Research Experiences for Undergraduates Summer Site Program to Florida Tech.

References

- Althaus, L. G. & Benvenuto, O. G. 1997, MNRAS, 288, L35
 Beauchamp, A., Wesemael, F., Bergeron, P., Fontaine, G., Saffer, R. A., Liebert, J., & Brassard, P. 1999, ApJ, 516, 887

- Bradley, P. A. 2002, in “Radial and Nonradial Pulsations as Probes of Stellar Physics”, eds. C. Aerts, T.R. Bedding, and J. Christensen-Dalsgaard, ASP Conference Series, 259, 382
- Bradley, P. A. & Winget, D. E. 1994, ApJ, 430, 850
- Brassard, P., & Fontaine, G. 2002, in White Dwarfs, ed. Martino, D., Silvotti, R., Solheim, J.-E., & Kalytis, R. (Dordrecht: Kluwer), in press.
- Breger, M. et al. 1993, A&A, 271, 482
- Brickhill, A. J. 1992, MNRAS, 259, 529
- Brickhill, A. J. 1991, MNRAS, 251, 673
- Brickhill, A. J. 1990, MNRAS, 246, 510
- Buchler, J. R., Goupil, M.-J., & Hansen, C. J. 1997, A&A, 321, 159
- Canuto, V. M., Goldman, I., & Mazzitelli, I. 1996, ApJ, 473, 550
- Clemens, J. C., van Kerkwijk, M. H., & Wu, Y. 2000, MNRAS, 314, 220
- Dehner, B. T. & Kawaler, S. D. 1995, ApJ, 445, L141
- Fontaine, G. & Brassard, P. 2002, ApJ, 581, L33
- Gautschi, A. & Althaus, L. G. 2002, A&A, 382, 141
- Goldreich, P. & Wu, Y. 1999a, ApJ, 511, 904
- Goldreich, P. & Wu, Y. 1999b, ApJ, 523, 805
- Ising, J. & Koester, D. 2001, A&A, 374, 116.
- Kawaler, S. D., Sekii, T., & Gough, D. 1999, ApJ, 516, 349
- Kepler, S. O. 1984, ApJ, 286, 314
- Kepler, S. O. 1993, Baltic Astronomy, 2, 515
- Kleinman, S. J., Nather, R. E. & Phillips, T. 1996, PASP, 108, 356
- Kleinman, S. J. et al. 1998, ApJ, 495, 424
- Kotak, R., van Kerkwijk, M. H., Clemens, J. C., & Koester, D. 2002, *in press* (astro-ph 021691)
- Kuschnig, R., Weiss, W. W., Gruber, R., Bely, P. Y., & Jenkner, H. 1997, A&A, 328, 544
- Metcalfe, T. S. & Charbonneau, P. 2003, J. Comp. Phys., in press.
- Metcalfe, T. S., Winget, D. E., & Charbonneau, P. 2001, ApJ, 557, 1021
- Metcalfe, T. S., Salaris, M., & Winget, D. E. 2002, ApJ, 573, 803
- Montgomery, M. H., Metcalfe, T. S., & Winget, D. E. 2001, ApJ, 548, L53
- Nather, R. E., Winget, D. E., Clemens, J. C., Hansen, C. J., & Hine, B. P. 1990, ApJ, 361, 309
- Provencal, J. L., Shipman, H. L., Thejll, P., & Vennes, S. J. 2000, ApJ, 542, 1041
- Robinson, E. L., Kepler, S. O., & Nather, R. E. 1982, ApJ, 259, 219
- Scargle, J. D. 1982, ApJ, 263, 835
- Schwarzenberg-Czerny, A. 1991, MNRAS, 253, 198
- Schwarzenberg-Czerny, A. 1999, ApJ, 516, 315
- Shipman, H. L., Provencal, J., Riddle, R., Vuckovic, M. 2002, AAS, 200, 7206.
- Standish, E. M. 1998, A&A, 336, 381
- Thompson, S.E., Clemens, J. C., van Kerkwijk, M. H., & Koester, D. 2003, ApJ, submitted.
- van Kerkwijk, M. H., Clemens, J. C., & Wu, Y. 2000, MNRAS, 314, 209
- Vuille, F. et al. 2000, MNRAS, 314, 689
- Winget, D. E. et al. 1994, ApJ, 430, 839
- Winget, D. E., Robinson, E. L., Nather, R. E., Kepler, S. O., & O’Donoghue, D. 1985, ApJ, 292, 606
- Wolff, B., Koester, D., Montgomery, M. H., & Winget, D. E. 2002, A&A, 388, 320
- Wu, Y. 2001, MNRAS, 323, 248
- Wu, Y., & Goldreich, P. 2001, ApJ, 546, 469

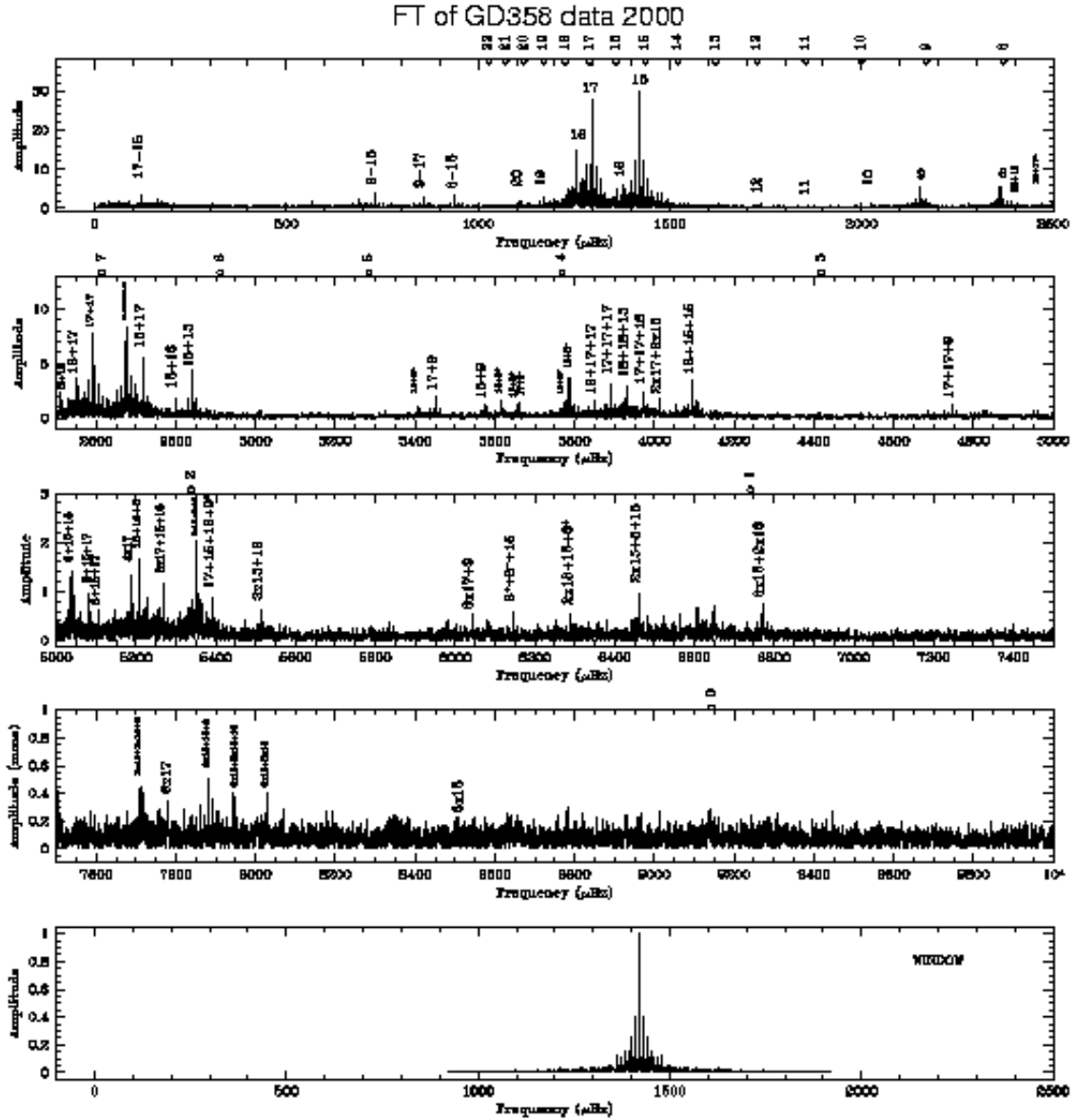


Fig. 1. Fourier transform of the 2000 data set. The main power is concentrated in the region between $1000 \mu\text{Hz}$ and $2500 \mu\text{Hz}$. The marks on top of the graph are the asymptotic equally spaced periods prediction, and the numbers represent the radial order k value, with Winget et al. (1994) identification. The vertical scale on each panel are adjusted to accommodate the large range of amplitudes shown, and the noise level which decreases from 0.29 mma up to $3000 \mu\text{Hz}$ to 0.19 mma upwards.

Table 11. Linear Combination of Peaks in 2000

k	Period (s)	Amp. (mma)	f_{obs} (μ Hz)	Combination	f_{comb} (μ Hz)	$\Delta f = f_{obs} - f_{comb}$ (μ Hz)
	8096.02	3.518	123.52	15 – 17	123.49	0.02
”	”	”	”	16 – $\ell = 2$	123.38	0.14
”	”	”	”	17 – 19	123.61	-0.09
	6078.39	2.169	164.52	15 – 18	164.68	-0.17
	6032.23	1.340	165.78	15 – 18 ^f	165.65	0.12
	5669.64	1.152	176.38			
	1765.91	1.738	566.28	11 – 17	566.27	0.01
	1539.52	1.009	649.56			
	1450.02	2.140	689.64	11 – 19	689.88	-0.23
	1369.15	3.584	730.38	10 – 17	730.40	-0.02
	1289.88	0.881	775.26	9 ⁰ – 16	775.23	0.03
	1166.29	2.876	857.42	9 ⁰ – 17	857.42	0.00
	1064.99	3.162	938.97	8 ⁺ – 15	939.02	-0.04
	1056.84	1.121	946.22	8 ⁻ – 15	946.17	0.04
	959.37	0.977	1042.35	9 ⁰ – 20	1043.07	-0.72
	941.28	0.895	1062.39	8 ⁺ – 17	1062.51	-0.12
	900.84	1.401	1110.07	8 ⁻ – $\ell = 2^a$	1110.03	0.05
20	900.13	2.029	1110.95	8 ⁻ – $\ell = 2$	1110.86	0.10
	853.57	1.816	1171.55			
19	852.52	2.740	1172.99			
$\ell = 2^b?$	798.80	3.662	1251.87	$\ell = 2 - 3.54\mu$ Hz		
$\ell = 2^g?$	797.63	5.858	1253.72			
$\ell = 2^f?$	797.17	5.330	1254.44			
$\ell = 2$	796.55	14.870	1255.41	not 1235 μ Hz		
$\ell = 2^a?$	796.02	7.508	1256.24			
$\ell = 2^b?$	795.73	1.280	1256.71			
$\ell = 2^c?$	795.36	3.277	1257.29	$\ell = 2 + 1.88\mu$ Hz		
$\ell = 2^d?$	794.75	2.433	1258.26	18 $\ell = 2 + 2.85\mu$ Hz		
$\ell = 2^e?$	793.88	1.568	1259.63	18 $\ell = 2 + 4.22\mu$ Hz		
	782.89	1.546	1277.31			
	781.92	1.350	1278.90			
17 ^a	771.68	1.221	1295.87			
17	771.25	27.940	1296.60			
17 ^b	770.80	1.604	1297.36			
	759.39	1.205	1316.85			
	725.70	1.286	1377.98	7 – 17 ^b	1378.13	-0.15
16	725.27	5.157	1378.80	15 + 18 $\ell = 2 - 17$	1378.76	0.03
	724.78	2.688	1379.73			
	709.03	1.185	1410.38			
15 ⁺	704.18	29.720	1420.10			
15 ^a	702.44	3.003	1423.62	15+3.52 μ Hz		
	690.99	1.123	1447.21			
12	575.94	1.030	1736.29			
11	536.81	0.830	1862.87			
10	493.34	1.280	2027.00			
9 ⁺	465.01	2.980	2150.49	9+3.54 μ Hz		
9 ⁰	464.25	5.300	2154.03			
9 ⁻	463.45	2.510	2157.72	9-3.69 μ Hz		
	447.30	0.968	2235.66	17 + 8 ⁺ – 15 ⁺	2235.61	0.08
	439.08	0.989	2277.50	15 ⁺ + 9 – 17	2277.53	-0.02

k	Period (s)	Amp. (mma)	f_{obs} (μ Hz)	Combination	f_{comb} (μ Hz)	$\Delta f = f_{obs} - f_{comb}$ (μ Hz)
8 ⁺	423.89	5.640	2359.11			
8 ⁻	422.61	5.620	2366.27	8 ⁺ - 2 \times 3.58 μ Hz		
	415.34	1.030	2407.65	20 + 17	2407.56	0.09
	405.15	1.388	2468.21	19 + 17 ^a	2468.86	-0.65
	404.89	1.091	2469.83	19 + 17	2469.60	0.24
	398.57	1.249	2508.96	2 \times $\ell = 2^f$	2508.89	0.08
	398.29	1.423	2510.74	2 \times $\ell = 2$	2510.83	-0.09
	398.15	2.052	2511.65	2 \times $\ell = 2^a$	2512.49	-0.84
	392.10	1.670	2550.34	$\ell = 2^g + 17$	2550.32	0.01
	392.00	1.737	2551.04	$\ell = 2^g + 17^b$	2551.08	-0.04
"	"	"	"	$\ell = 2^f + 17$	2551.05	0.00
"	"	"	"	$\ell = 2 + 17^a$	2551.28	-0.24
	391.85	3.703	2552.02	19 + 16	2551.79	0.23
"	"	"	"	$\ell = 2^f + 17^a$	2551.80	0.22
"	"	"	"	$\ell = 2 + 17$	2552.02	0.00
"	"	"	"	$\ell = 2^a + 17^a$	2552.11	-0.09
	391.72	2.007	2552.83	$\ell = 2 + 17^b$	2552.77	0.05
"	"	"	"	$\ell = 2^a + 17$	2552.85	-0.02
"	"	"	"	$\ell = 2^b + 17^a$	2552.58	0.24
"	"	"	"	$\ell = 2^c + 17$	2553.32	-0.49
"	"	"	"	$\ell = 2^c + 17^a$	2553.16	-0.34
	391.56	1.159	2553.88	$\ell = 2^a + 17^b$	2553.60	0.28
"	"	"	"	$\ell = 2^b + 17^b$	2554.07	-0.19
"	"	"	"	$\ell = 2^c + 17$	2553.90	-0.02
"	"	"	"	$\ell = 2^c + 17^b$	2554.65	-0.77
"	"	"	"	$\ell = 2^e + 17^a$	2554.13	-0.25
	385.62	7.759	2593.21	2 \times 17	2593.21	0.00
	379.48	0.928	2635.16	$\ell = 2 + 16$	2634.21	0.95
"	"	"	"	$\ell = 2^a + 16$	2635.04	0.12
"	"	"	"	$\ell = 2^b + 16$	2635.51	-0.35
	374.24	1.576	2672.05	19 ^a + 15	2671.97	0.08
	374.00	3.459	2673.81	$\ell = 2^g + 15$	2673.82	-0.01
	373.89	3.498	2674.56	$\ell = 2^f + 15$	2674.54	0.02
"	"	"	"	17 ^a + 16	2674.67	-0.10
7	373.76	8.430	2675.49	17 + 16	2675.40	0.09
	373.64	4.254	2676.40	$\ell = 2^a + 15$	2676.34	0.06
"	"	"	"	$\ell = 2^b + 15$	2676.81	-0.41
"	"	"	"	17 ^b + 16	2676.15	0.25
	373.50	1.827	2677.38	$\ell = 2^g + 15^a$	2677.34	0.04
"	"	"	"	$\ell = 2^c + 15$	2677.39	-0.01
	373.38	1.193	2678.22	$\ell = 2^g + 15^a$	2678.06	0.16
"	"	"	"	$\ell = 2^e + 15$	2678.35	-0.13
	373.16	0.870	2679.78	$\ell = 2 + 15^a$	2679.03	0.75
"	"	"	"	$\ell = 2^a + 15^a$	2679.86	-0.08
"	"	"	"	$\ell = 2^b + 15^a$	2680.33	-0.55
	372.83	0.932	2682.18	15 ^a + $\ell = 2^d$	2681.87	0.30
	368.09	5.653	2716.71	17 + 15	2716.70	0.01
	367.62	0.840	2720.17	17 ^a + 15 ^a	2719.49	0.68
"	"	"	"	17 + 15 ^a	2720.22	-0.05
	357.29	1.731	2798.86	16 + 15	2798.89	-0.03
	357.16	0.877	2799.88	16 ^a + 15	2799.83	0.05

k	Period (s)	Amp. (mma)	f_{obs} (μ Hz)	Combination	f_{comb} (μ Hz)	$\Delta f = f_{obs} - f_{comb}$ (μ Hz)
	352.09	4.260	2840.20	2×15	2840.19	0.01
	351.66	1.054	2843.68	$15 + 15^a$	2843.71	-0.03
	293.60	0.992	3405.99	$\ell = 2 + 9^+$	3405.91	0.09
"	"	"	"	$\ell = 2^a + 9^+$	3406.74	-0.74
"	"	"	"	$16 + 10$	3405.79	0.20
	289.80	1.929	3450.64	$17^a + 9^0$	3449.90	0.74
"	"	"	"	$17 + 9^0$	3450.63	0.01
"	"	"	"	$15^a + 10$	3450.62	0.02
	279.78	1.393	3574.19	$15 + 9^0$	3574.12	0.07
"	"	"	"	$15^a + 9^+$	3574.11	0.08
	279.50	1.118	3577.77	$15 + 9^-$	3577.82	-0.05
"	"	"	"	$15^a + 9^0$	3577.65	0.13
	276.66	1.550	3614.54	$\ell = 2 + 8^+$	3614.53	0.01
	276.10	0.960	3621.85	$\ell = 2 + 8^-$	3621.68	0.17
	273.54	1.284	3655.77	$17 + 8^+$	3655.72	0.05
	273.01	1.382	3662.91	$17 + 8^-$	3662.87	0.03
	264.60	1.523	3779.25	$15 + 8^+$	3779.21	0.04
	264.11	3.649	3786.37	$15 + 8^-$	3786.37	0.00
"	"	"	"	$20 + 7$	3786.44	-0.07
	259.84	1.569	3848.54	$19 + 7$	3848.48	0.06
	259.78	0.885	3849.36	$2 \times 17 + \ell = 2$	3848.61	0.75
	257.08	3.204	3889.80	3×17	3889.81	-0.02
	254.51	1.744	3929.10	$\ell = 2^g + 7$	3929.21	-0.11
"	"	"	"	$\ell = 2 + \ell = 2^g + 15$	3929.22	-0.12
"	"	"	"	$15 + 2 \times \ell = 2^f$	3929.06	0.04
	254.42	1.140	3930.46	$\ell = 2^f + 7$	3929.93	0.53
"	"	"	"	$16 + \ell = 2 + 17^a$	3929.84	0.62
"	"	"	"	$15 + 2 \times \ell = 2$	3930.83	-0.37
	254.34	2.986	3931.77	$2 \times 17 + \ell = 2 + 16$	3931.76	0.00
	251.82	1.015	3971.17	$17 + \ell = 2^g + 15$	3970.41	0.75
"	"	"	"	$15 + \ell = 2^f + 17$	3970.44	0.73
"	"	"	"	$15 + \ell = 2 + 17^a$	3971.14	0.03
	251.76	2.242	3972.03	$15 + 17 + \ell = 2$	3972.12	-0.08
"	"	"	"	$16 + 2 \times 17$	3972.01	0.03
"	"	"	"	$17 + 7$	3972.09	-0.06
	251.70	1.395	3972.93	$17 + \ell = 2^a + 15$	3973.01	-0.07
"	"	"	"	$15 + 17^a + 16$	3972.92	0.01
	249.17	1.822	4013.33	$2 \times 17 + 2 \times 15$	4013.31	0.02
	246.59	0.948	4055.26	$15 + 16 + \ell = 2$	4055.26	0.00
	244.27	1.462	4093.91	$15 + 2 \times \ell = 2$	4093.90	0.01
	244.22	1.576	4094.67	$\ell = 2^g + 2 \times 15$	4094.64	0.03
"	"	"	"	$17^a + 16 + 15$	4094.73	-0.06
"	"	"	"	$2 \times 15 + \ell = 2^f$	4094.66	0.02
	244.16	3.487	4095.59	$\ell = 2 + 2 \times 15$	4095.61	-0.02
"	"	"	"	$17 + 16 + 15$	4095.47	0.12
"	"	"	"	$15 + 7$	4095.58	0.01
	244.11	1.722	4096.45	$17 + 15 + 16^a$	4096.48	-0.03
"	"	"	"	$16 + 17^a + 16$	4096.50	-0.05
	210.65	1.196	4747.23	$2 \times 17 + 9^0$	4747.24	-0.01
	198.63	1.272	5034.61	$15 + \ell = 2 + 8^+$	5034.64	-0.03
	198.34	1.451	5041.82	$15 + \ell = 2 + 8^-$	5041.95	-0.14

k	Period (s)	Amp. (mma)	f_{obs} (μ Hz)	Combination	f_{comb} (μ Hz)	$\Delta f = f_{obs} - f_{comb}$ (μ Hz)
	196.74	0.992	5082.98	$17 + 15 + 8^-$	5082.97	0.00
	192.81	1.319	5186.46	4×17	5186.42	0.04
"	"	"	"	$3 \times \ell = 2 + 15$	5185.88	0.59
"	"	"	"	$2 \times \ell = 2 + 16 + 17$	5187.18	-0.72
	192.07	1.641	5206.47	$2 \times 15 + 8^-$	5206.47	0.00
	189.81	1.171	5268.55	$2 \times 17 + 7$	5267.77	0.78
"	"	"	"	$2 \times 17 + 15 + \ell = 2$	5268.64	-0.09
	186.94	1.153	5349.20	$3 \times \ell = 2 + 15$	5349.33	-0.12
	186.85	2.004	5351.84	2×7	5350.97	0.87
"	"	"	"	$15 + 16 + 17 + \ell = 2$	5351.86	-0.02
	185.46	0.842	5392.02	$2 \times 15 + 17 + \ell = 2$	5392.13	-0.11
	181.30	0.609	5515.65	$3 \times 15 + \ell = 2$	5515.69	-0.04
	165.46	0.533	6043.85	$15 + 17 + \ell = 2 + 9^0$	6043.83	0.01
	162.72	0.584	6145.42	$8^+ + 8^- + 15$	6145.48	-0.07
	158.96	0.554	6290.83	$2 \times \ell = 2 + 15 + 8^+$	6290.02	0.81
"	"	"	"	$8^+ + 16 + 17 + \ell = 2$	6290.88	-0.05
	154.76	0.958	6461.78	3×9^0	6462.08	-0.30
"	"	"	"	$\ell = 2 + 2 \times 15 + 8^-$	6461.88	-0.10
"	"	"	"	$16 + 15 + 17 + 8^-$	6461.77	0.01
	147.67	0.761	6771.90	$2 \times \ell = 2 + 3 \times 15$	6771.06	0.84
"	"	"	"	$2 \times \ell = 2 + 15 + 16 + 17$	6771.94	-0.04
	129.69	0.438	7710.99	$2 \times 15 + 8^+ + 8^-$	7710.93	0.06
"	"	"	"	$8^+ + 15 + 16 + 17 + \ell = 2$	7710.95	0.04
"	"	"	"	$7 + 8^+ + 15 + \ell = 2$	7710.10	0.89
	129.61	0.410	7715.61	$8^- + 3 \times \ell = 2 + 15$	7715.47	0.14
	126.87	0.502	7881.92	$3 \times 15 + \ell = 2 + 8^+$	7881.87	0.05
	125.87	0.410	7944.98	$2 \times 15 + 2 \times \ell = 2 + 2 \times 17$	7944.07	0.91
	124.56	0.401	8028.10	$3 \times \ell = 2 + 3 \times 15$	8027.31	0.78
"	"	"	"	$3 \times \ell = 2 + 15 + 16 + 17$	8027.31	0.78

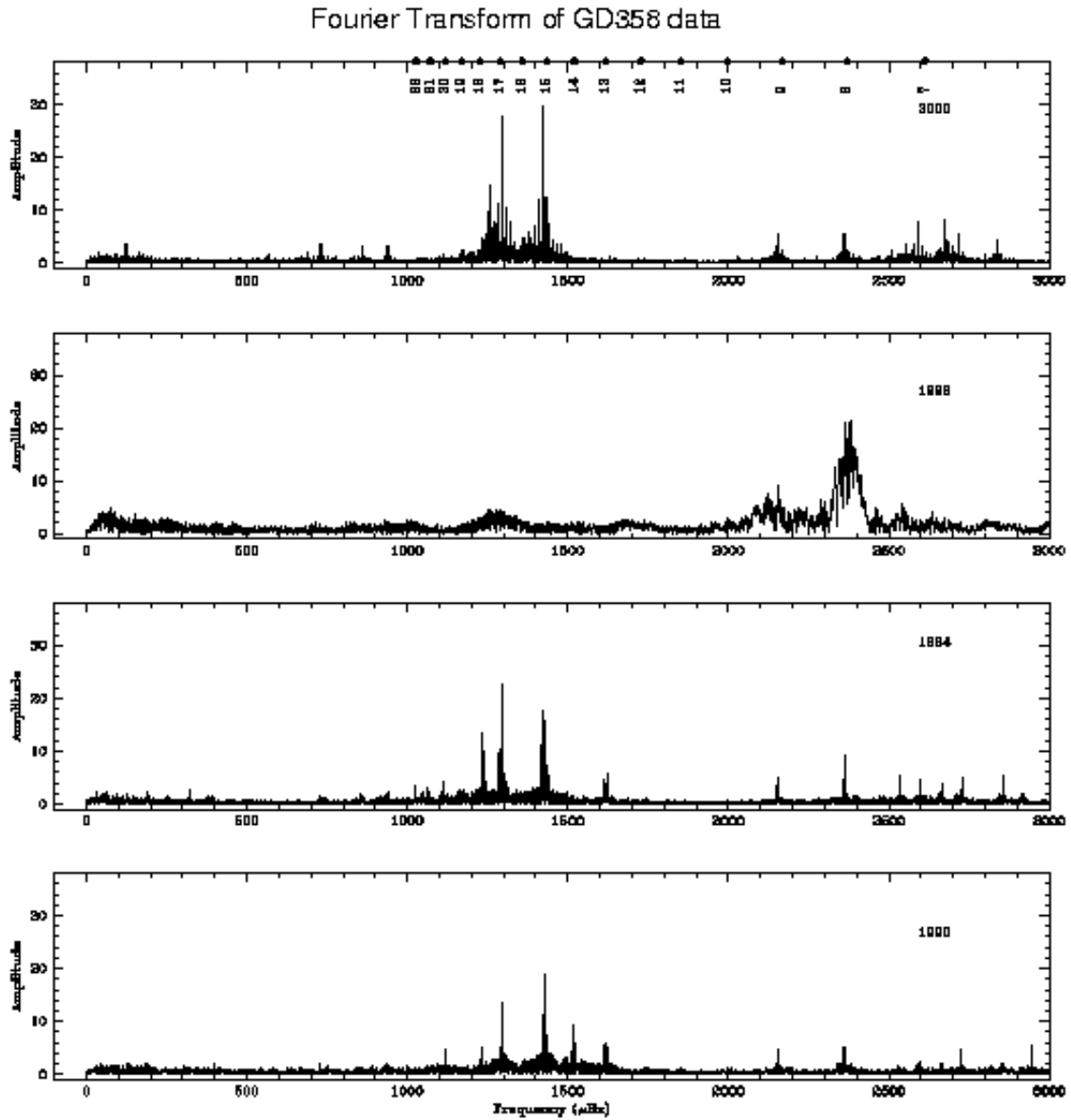


Fig. 2. Fourier transform of the GD 358 data, year by year.

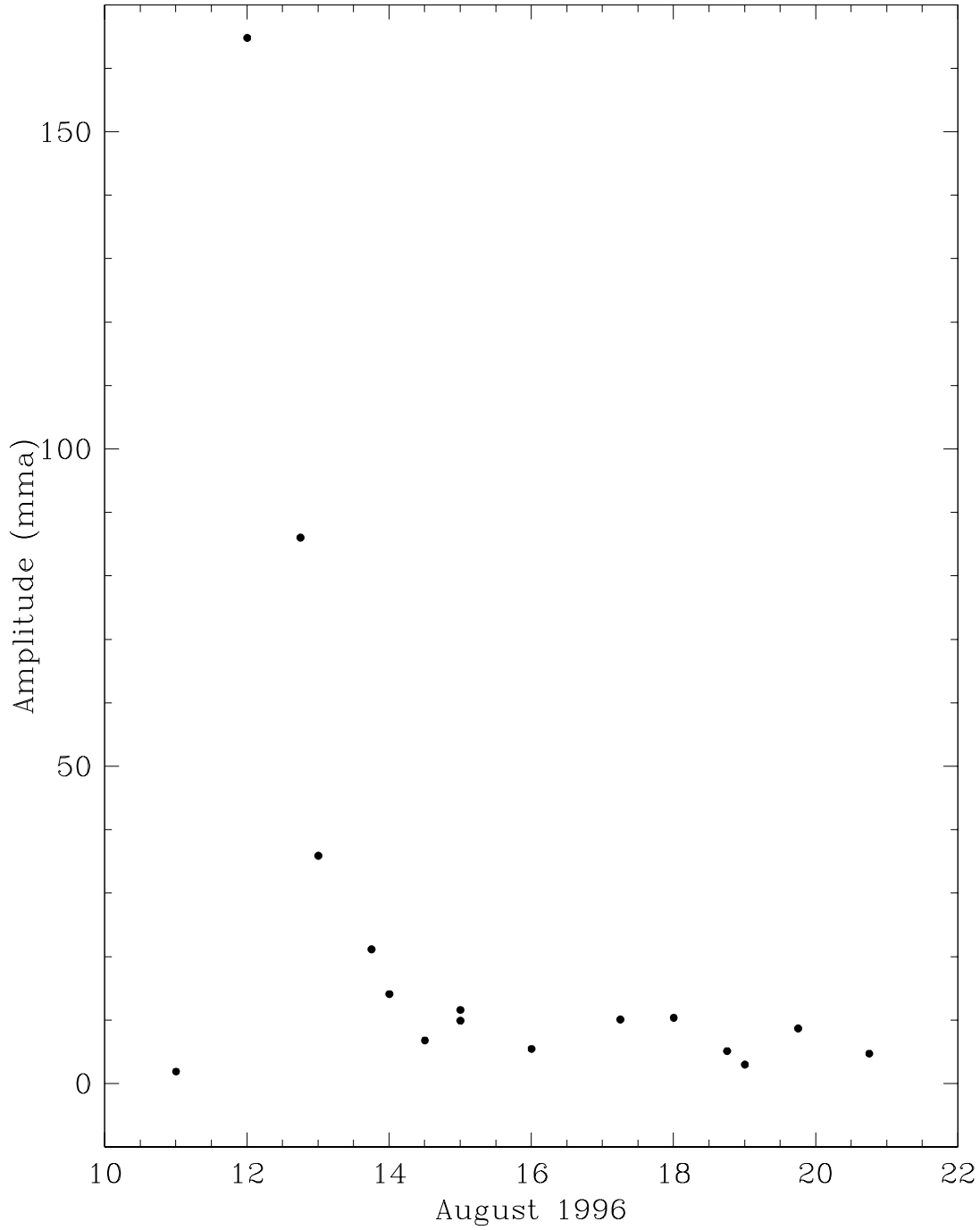


Fig. 3. The amplitude modulation of GD 358 423 s mode observed in the optical in August, 1996. The timescale of this change is surprisingly short. We have never observed such a fast amplitude modulation in any of the pulsating white dwarf stars.

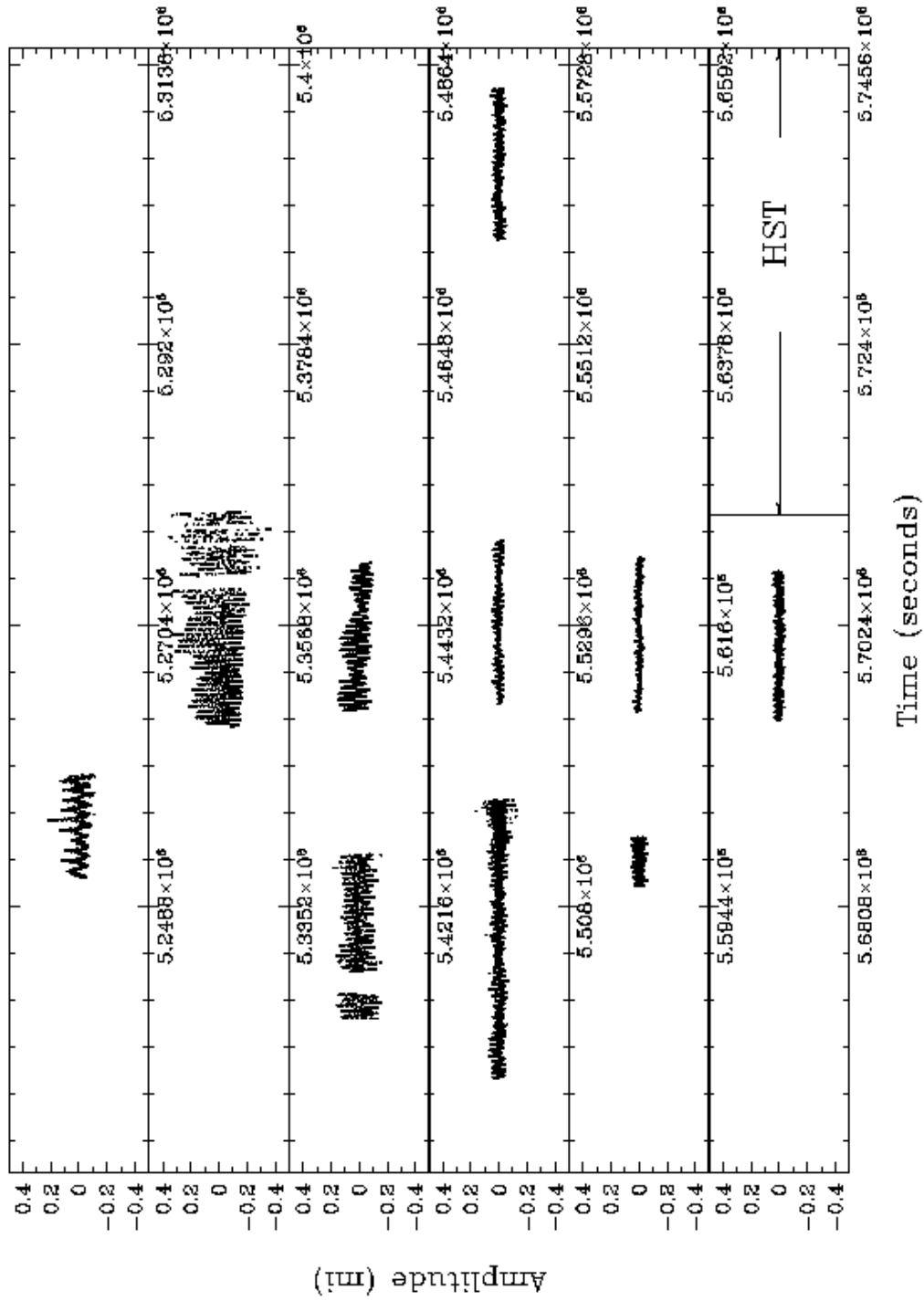


Fig. 4. First half of the ground-based optical lightcurve of GD 358 in August 1996. Each panel is one day long.

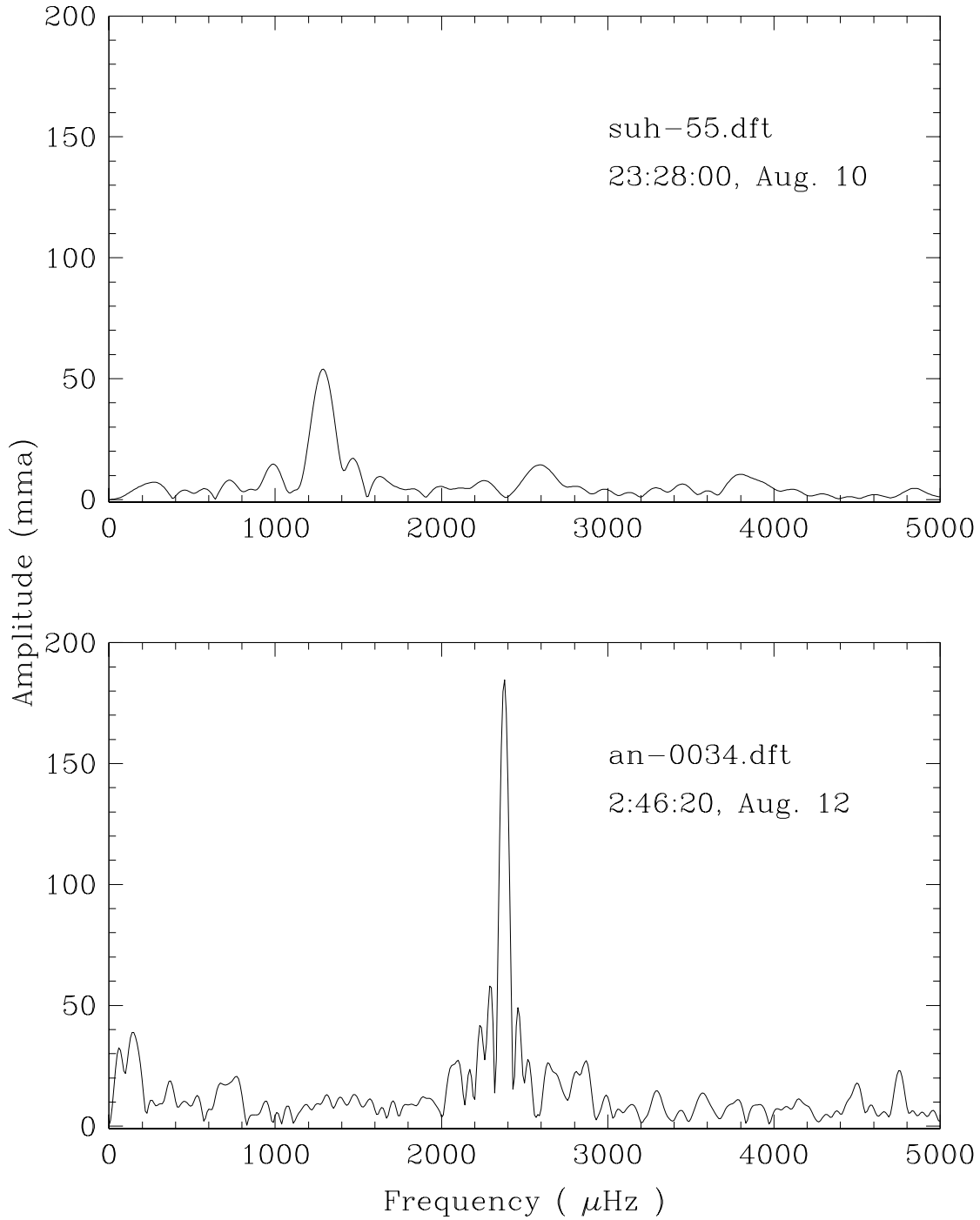


Fig. 5. Fourier transforms of GD 358 observed one day apart. The top panel shows the Fourier transform of the data taken on the 1st day of the 3-site campaign (suh-55: taken in Poland with start time at 23:28:00 UT on August 10), and the bottom panel shows the data taken about one day later from McDonald (an-0034: taken with start time at 2:48:20 UT on August 12). The observed power has shifted completely and dramatically, both in frequency and amplitude.

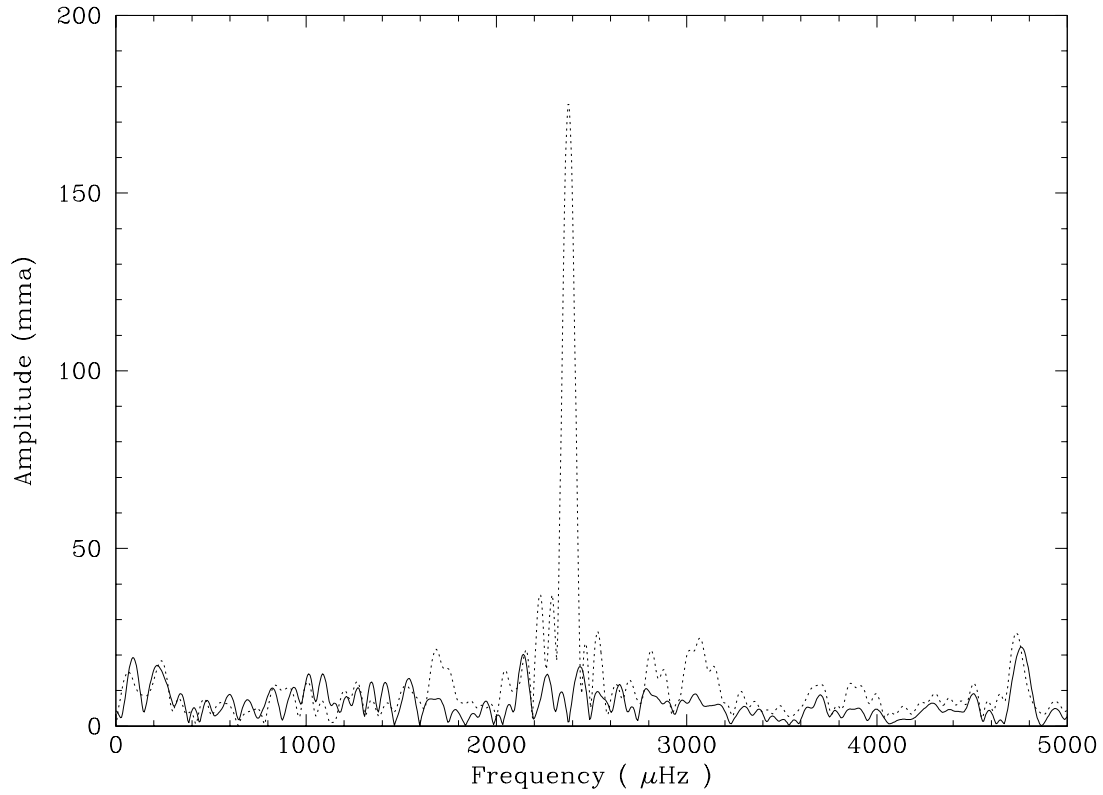


Fig. 6. Fourier transform of an-0034 before (dotted line) and after (solid line) it was prewhitened by the 423 s mode. After prewhitening, there is little significant power left. The lightcurve was dominated by one mode, a possible explanation for why the lightcurve looked so linear (sinusoidal) in Fig. 4.

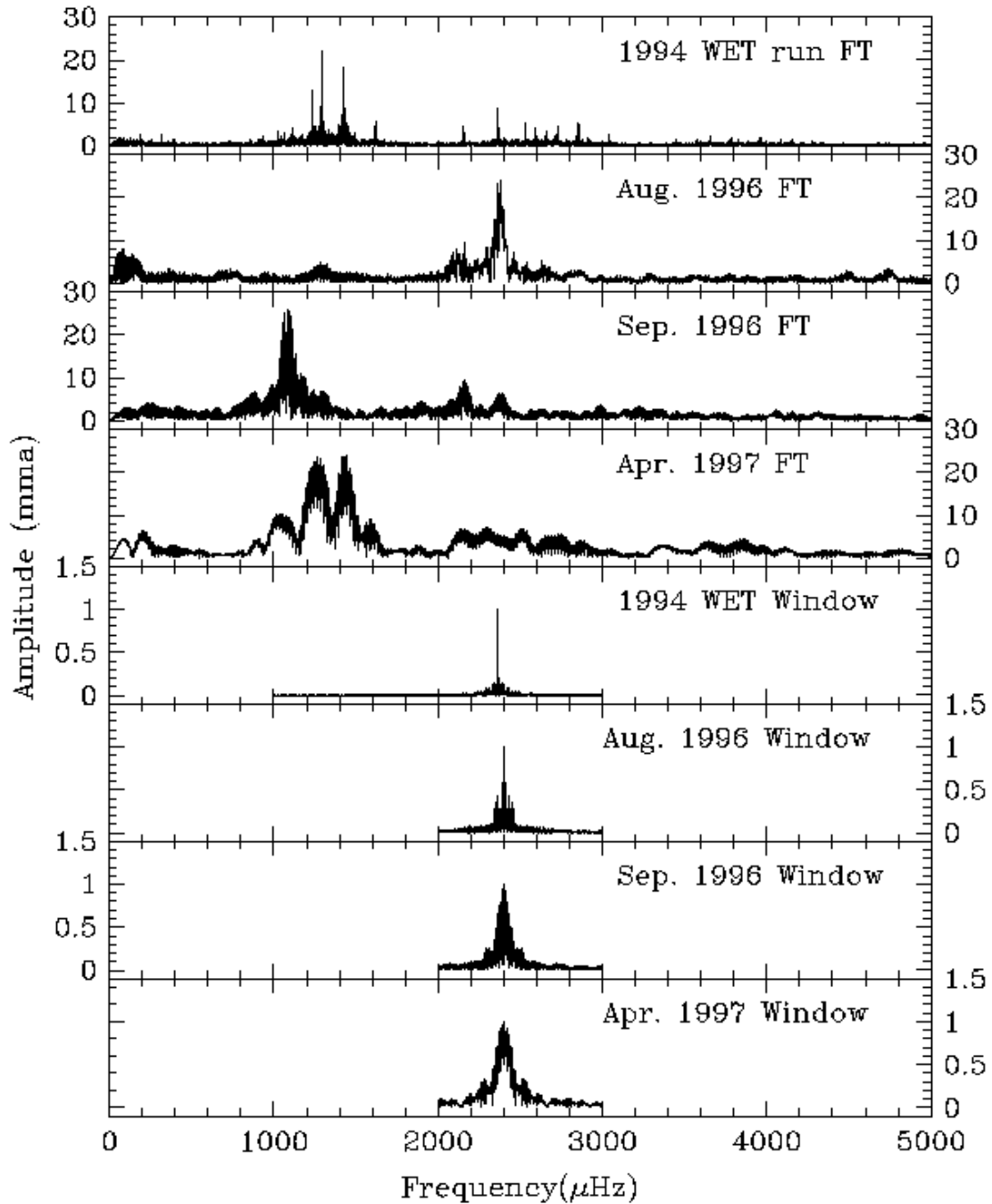


Fig. 7. GD 358 Fourier transform at four different times along with their spectral windows. The 1994 and 1997 Fourier transforms look similar (within the observed frequency resolution, that is). The September 1996 data look similar as well to these two data sets, but the highest amplitude modes have shorter frequencies (longer period). Obviously, the August 1996 Fourier transform looks very different from the other Fourier transforms.

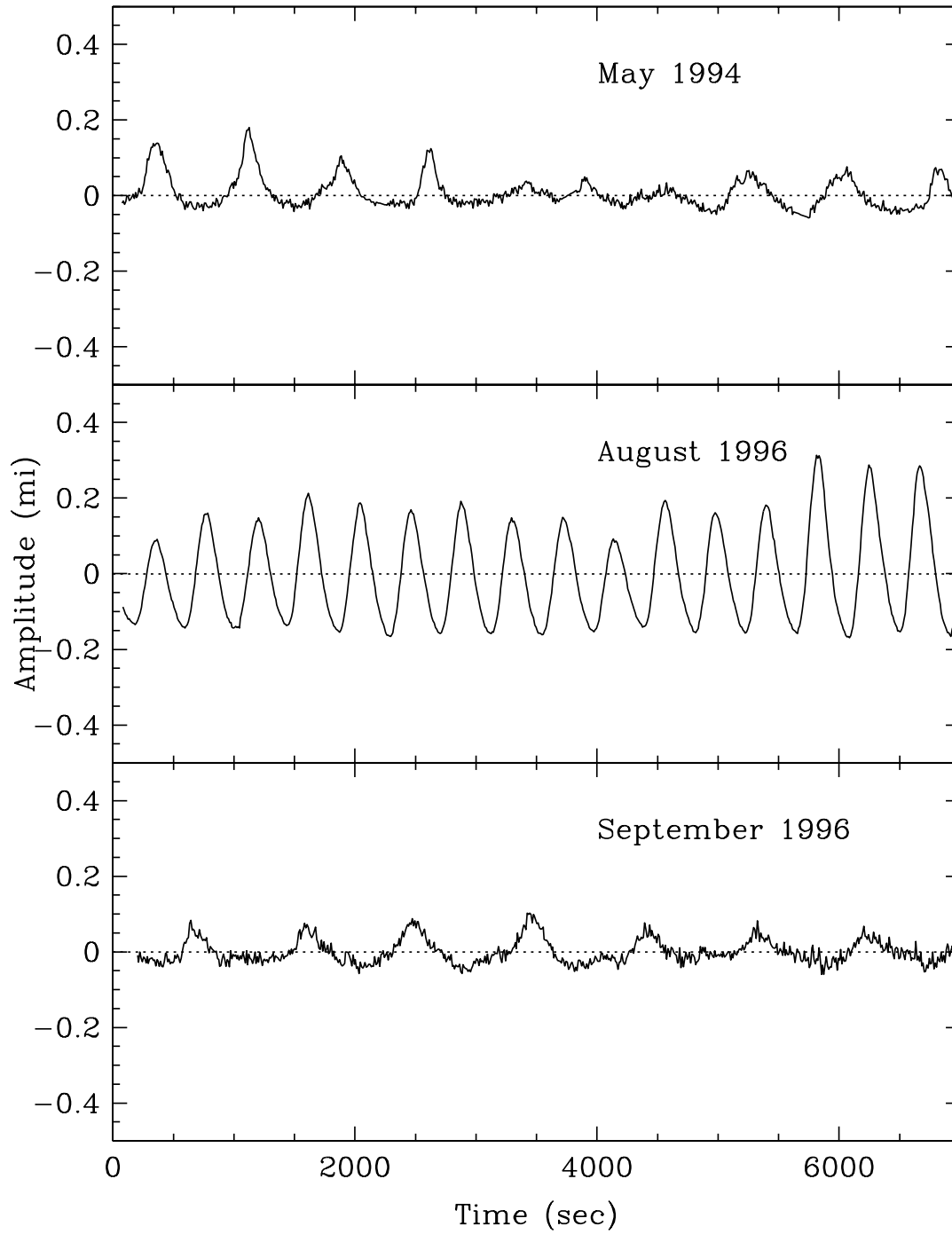


Fig. 8. GD 358 lightcurves over time. The shape of the lightcurve was sinusoidal when the amplitude was highest. The 1994 and September 1996 data exhibit similar pulse shapes and their corresponding power spectra also look similar (Fig. 7).

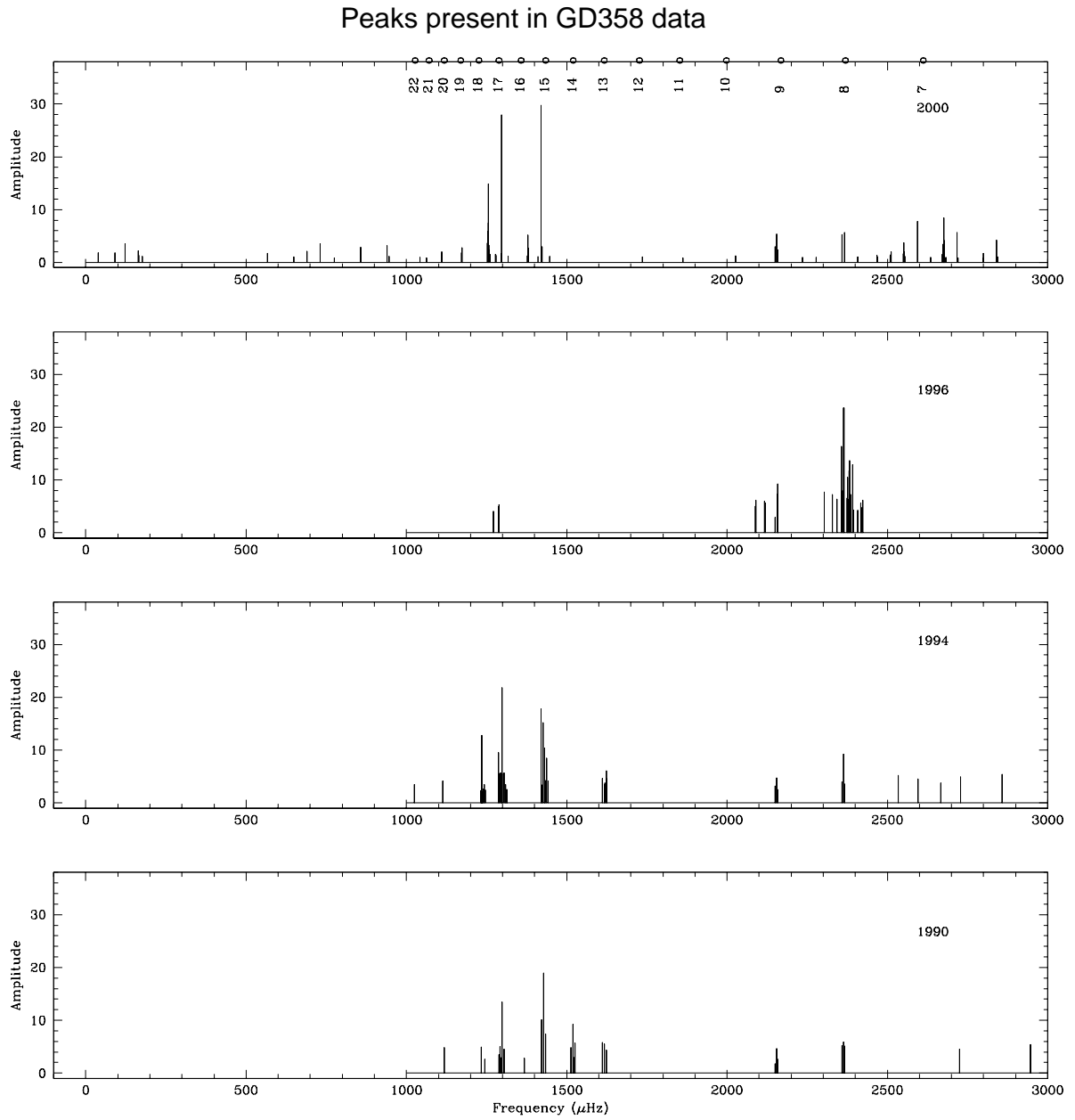


Fig. 10. Results of pre-whitening for the 1990, 1994, August 1996, and 2000 data sets

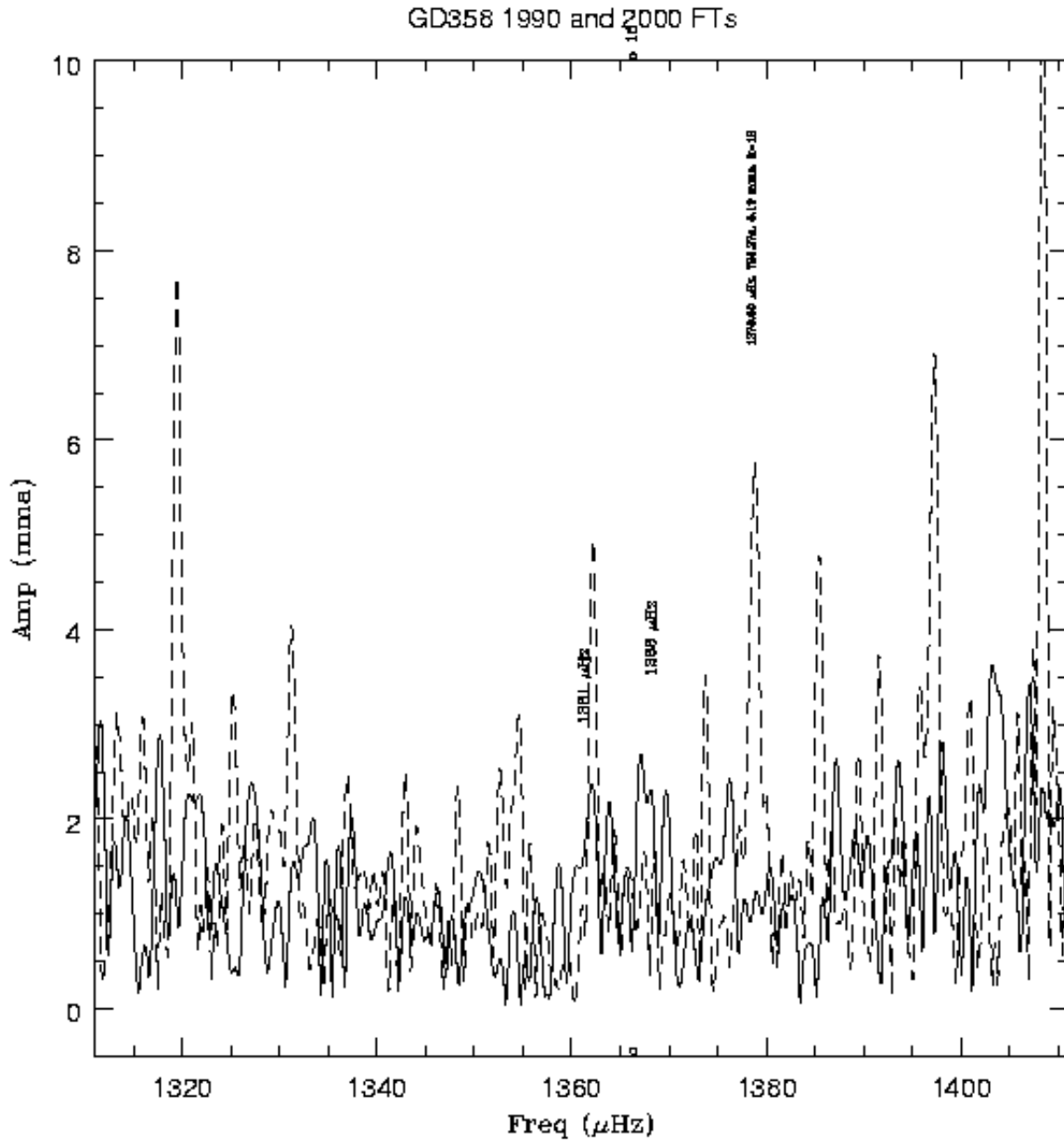


Fig. 11. Peaks around $k=16$ in the 1990 (solid line) and 2000 (dashed line) transforms

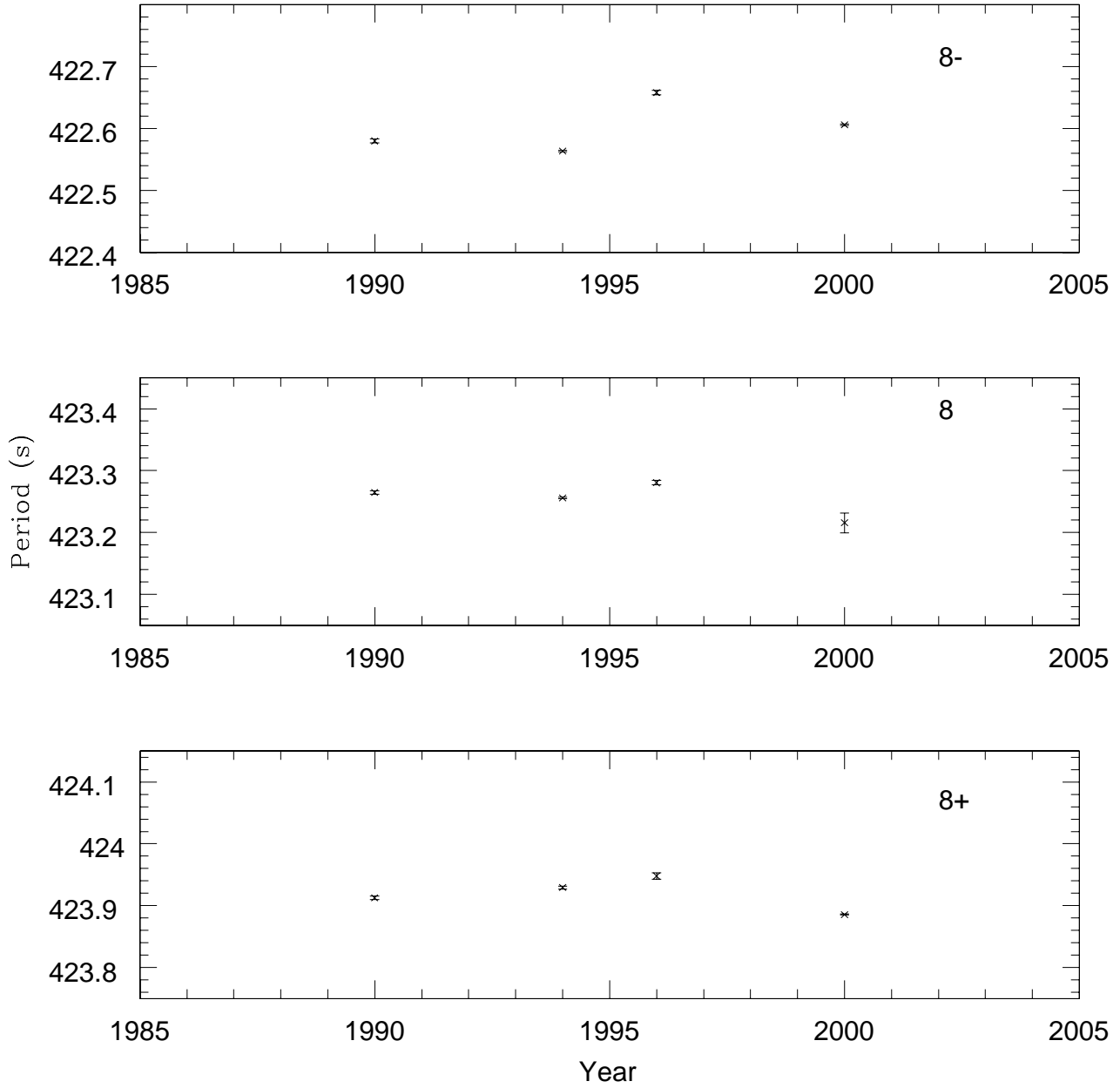


Fig. 12. Search for \dot{P} : The periods of the m subcomponents of even the most stable mode, $k = 8$, change significantly, from year to year. The same behavior is detected for all pulsations.

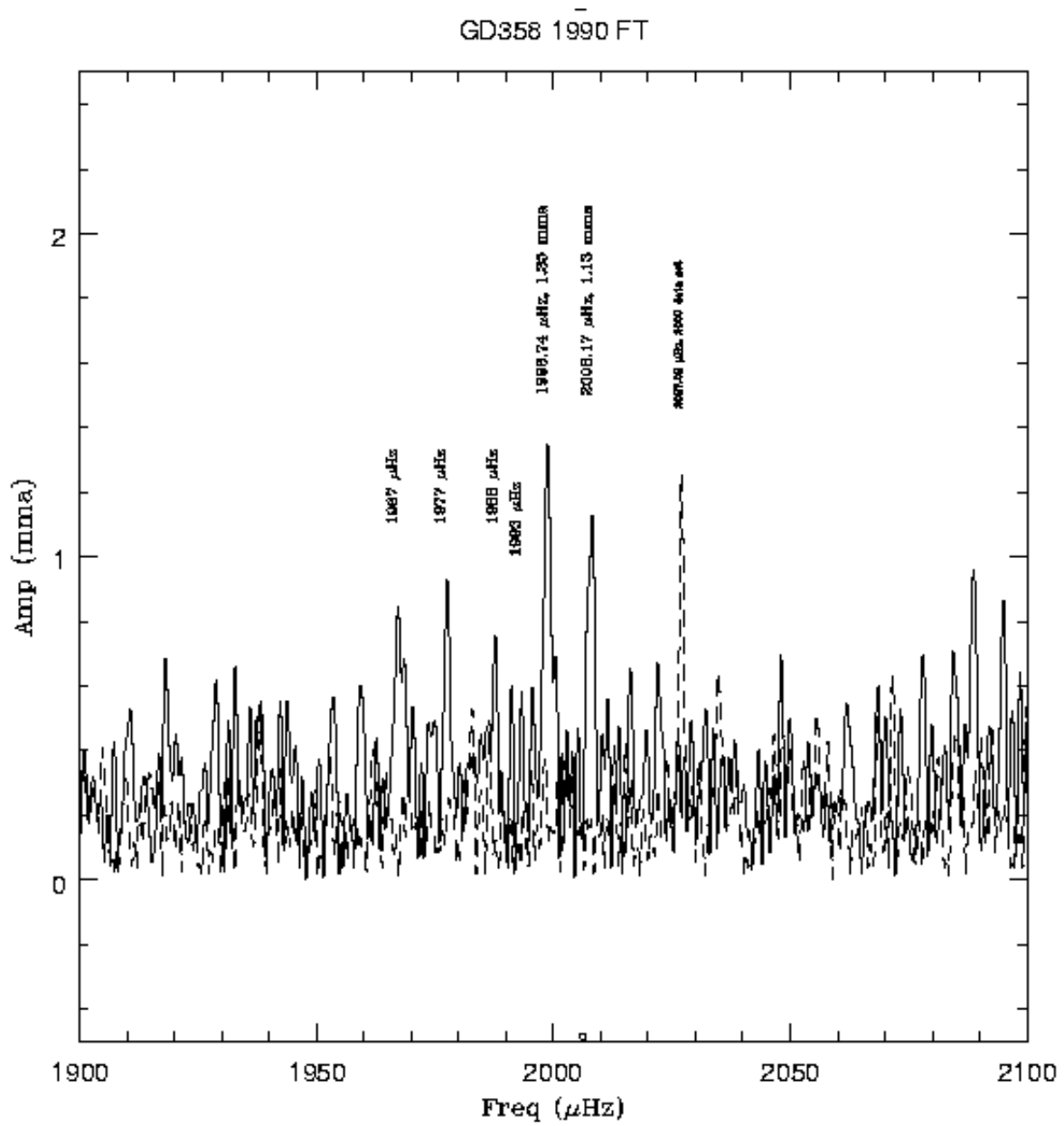


Fig. 13. Peaks around $k=10$ in the 1990 (solid line) and 2000 (dashed line) transforms

